2023-12

Optimal control and cost effectiveness analysis of contamination associated with aflatoxins in maize kernels, livestock and humans

Mgandu, Filimon

Elsevier

https://doi.org/10.1016/j.rico.2023.100313

Results in Control and Optimization 13 (2023) 100313

Contents lists available at ScienceDirect

Results in Control and Optimization

journal homepage: www.elsevier.com/locate/rico

Optimal control and cost effectiveness analysis of contamination associated with aflatoxins in maize kernels, livestock and humans

F.A. Mgandu [a,b,*], S. Mirau [a], N. Nyerere [c], F. Chirove [d]

[a] School of Computational and Communication Science and Engineering, The Nelson Mandela Institution of Science and Technology, P.O. Box 447, Arusha, Tanzania
[b] Department of ICT and Mathematics, College of Business Education, P.O. Box 2077, Dodoma, Tanzania
[c] Department of Mathematics and Statistics, Sokoine University of Agriculture, P.O. Box 3038, Morogoro, Tanzania
[d] Department of Mathematics and Applied Mathematics, University of Johannesburg, P.O. Box 524, Auckland Park, South Africa

ARTICLE INFO

Keywords:
Aflatoxin contamination
Optimal control
Cost effectiveness

ABSTRACT

Aflatoxin contamination poses a significant challenge in food safety and security as it affects both health of consumers and supply chains. Due to health impacts associated with aflatoxin contamination, countries have set standards and restrictions for importing food crops and animal feed, resulting in greater economic losses to farmers, transporters, and crop processors. Three controls, namely good farming practices, biological control and public education and awareness campaigns, have been mostly used in countries where aflatoxin contamination has occurred. Since resources are scarce, there is a need to find the optimal and cost-effective strategy to reduce the burden on farmers. This study aimed to find optimal and cost-effective control strategy to mitigated aflatoxin contamination in maize kernels, livestock and humans. A deterministic model was developed and analyzed for studying the impact of implementing three time dependent controls on the dynamics and control of aflatoxin contamination in maize kernels, livestock and humans. We use optimal control theory to find the necessary conditions for existence of the optimal controls and to determine the optimal strategy for controlling the aflatoxin contamination. We also carry out cost-effectiveness analysis through Incremental Cost Effective Ratio (ICER) to obtain the most effective strategy. Simulation results for the optimal control problem suggest that strategy which involve implementation of all controls performs well than other strategies in controlling the aflatoxin contamination in maize kernels, livestock and humans. Therefore, to control aflatoxin contamination initiatives should focus on good farming practices, biological control and public education and awareness campaigns.

1. Introduction

Aflatoxins are poisonous substances that are produced by *Aspergillus flavus* and *Aspergillus parasiticus* (certain types of fungi) that are found naturally all over the world and can grow in the soil, on decaying vegetation, and grains if conditions are favorable [1,2]. Temperatures around 30 °C [2], relative humidity between 80% and 85% [3], water activity between 0.81–0.99aw [4,5], soil pH at optimum range of 3 to 7 [6,7] and other factors are ideal for *Aspergillus* to grow and produce aflatoxin. There are more than 20 different types of aflatoxins, but the most important are B_1, B_2, G_1 and G_2 with aflatoxin B_1 being the most frequent in food crops and having greater toxin power [2,3,8,9]. When contaminated food is processed, aflatoxins enter the general food supply, where

* Corresponding author at: School of Computational and Communication Science and Engineering, The Nelson Mandela Institution of Science and Technology, P.O. Box 447, Arusha, Tanzania.
E-mail address: mganduf@nm-aist.ac.tz (F.A. Mgandu).

https://doi.org/10.1016/j.rico.2023.100313
Received 24 February 2023; Received in revised form 11 August 2023; Accepted 5 October 2023
Available online 12 October 2023

they can be found in both human food and feed for agricultural animals. Livestock fed on contaminated food can also pass aflatoxin into eggs, milk products and meat [10]. Humans get aflatoxin through consuming contaminated food, products of contaminated animals like meat, eggs, and milk products, or from mother to child through breastfeeding [11].

Aflatoxin contamination has been reported to have effects on the health of consumers and business chains. Consuming high doses of aflatoxin in a short period can cause acute aflatoxicosis, leading to death [12]. Intake of low to moderate doses of aflatoxins over a prolonged time period results in immunity suppression to all age groups, children's impaired growth and liver cancer [2,13,14]. Among these effects liver cancer is the most severe and well known [12]. Estimates show that among 782,200 new cases of liver cancer per year globally, more than 28.2% are associated with aflatoxin contamination, and 40% occurs in Africa [12,15,16]. Health impacts associated with aflatoxin contamination have forced countries to set standards and restrictions for importing food crops and animal feed, resulting in greater economic losses for farmers, transporters, and crop processors. For example, the European Union allows maize and groundnuts with below 5 $\mu g/kg$ and 8 $\mu g/kg$ aflatoxin concentrations respectively to be imported and consumed for food or feed [17]. The East African Community allows maize with below 10 $\mu g/kg$ to facilitate equal standard in importing and exporting maize among member countries [18]. The Food and Agriculture Organization of the United Nations (FAO) estimates that more than 25% of the world's food crops exceeds the aflatoxin standards and are destroyed each year [11,19,20]. It is estimated that aflatoxin contamination causes losses to the maize industry ranging from USD 52.1 million to USD 1.68 billion annually in the United States [21,22]. In Africa, Aflatoxin contamination cause losses of more than USD 750 millions annually [23,24].

Aflatoxin contamination in maize predominantly affects the maize kernels, which serve as a great source of nutrients for growth and aflatoxin production [25–28]. The aflatoxin-producing fungi grow and produce toxins on the surface of maize kernels before and after harvest that remain concentrated in the kernels. Aflatoxin-producing fungi can infect other parts of the maize plant, including the stems, leaves, and husks [29]. However, the concentration of aflatoxin is higher in the kernels, making them the primary concern when it comes to food safety and human health risks [25,29]. Since farmers and food processors are interested in storing maize kernels for future use, at any point, maize kernels will be in storage for a prolonged period of time, leading to post-harvest contamination. In our model, we are considering the average contamination rate of maize kernels from both pre- and post-harvest for simplicity.

Current control strategies in preventing aflatoxin contamination can be grouped into good agricultural practices, education and awareness, biological and physical control. The good agricultural practices that reduces aflatoxin contamination involve using resistant cultivars, crop rotation, weed and pest control, and proper drying and storage [20,30–32]. On education and awareness, people are required to take balanced and diversifying diets by reducing over consumption of most susceptible crops like maize and groundnuts [33]. The education and awareness also insist on proper feeding of livestock and avoiding more susceptible feed [33,34]. Biological control involves the use of atoxigenic fungi (non-aflatoxigenic) to competitively displace the toxigenic fungi (aflatoxigenic) for example Aflasafe [20,35]. Physical controls involve segregation, sorting, heating or cleaning contaminated crops [36,37].

Mathematical models can be used to study the dynamics of aflatoxin contamination from food crops to livestock and humans. With these models, different control strategies can be tested and simulated to ascertain their effectiveness before implementation. Models help to identify high and low risk areas based on historical data, the life cycle of aflatoxin-causing moulds, and environmental and weather factors. The types of mathematical models used range from empirical to mechanistic models [38,39]. Empirical models are based on statistical analysis of data observed in field experiments to establish the relationship between yields or aflatoxin contamination and climate variables. On the other hand, mechanistic models are based on cause-and-effect relationships among variables to represent biological, chemical, or physical process [38,39]. In practice, model development can involve both approaches.

The optimal control and cost-effectiveness analysis have been extensively used in dynamical systems to determine the best control strategies. We review a mathematical model for aflatoxin control using probiotics developed by [40] because it uses a system of ordinary differential equations and thus relates to our study. The model assumes an ecosystem where aflatoxin fungi and probiotics are placed together like a predator–prey system and the ability of probiotics to detoxify aflatoxin contamination is analyzed. Results from the model indicate that the ability of probiotics to detoxify depends on the rate of formation of the aflatoxin-probiotic complex. However, the study considered plants as one population, animals as one population and humans as one population which limited the exploration of incidents in each sub-population. Other studies in epidemiology have also employed optimal control and cost-effectiveness as well. Some recent interesting examples include co-infection models by [41–43], optimal control strategies for the infectiology of brucellosis [44], optimal control model for alcohol-related risk in Tanzania [45] and optimal control for the dynamics of COVID-19 disease in South Africa [46]. Other studies have used optimal control in time- or state-delayed dynamic systems. Interesting examples include studies by [47–49].

In this paper, we derive and analyze an aflatoxin contamination model with good farming practices, biological control and public education and awareness campaigns. We carry out an optimal control analysis of the model by employing the Pontryagins Maximum Principle to determine the optimal control strategies for controlling aflatoxin contamination. We apply the Incremental Cost-Effectiveness Ratio (ICER) technique to determine the most cost-effective strategy in controlling aflatoxin contamination.

The paper has the following structure: Section 2 contains model formulation, while Section 3 provides model analysis. Section 4 contains optimal control problem formulation and characterization. Section 5 shows numerical simulations, while Section 6 provides cost-effectiveness analysis for all control strategies. Lastly, the conclusion is presented in Section 7.

2. Model formulation

The model developed in this section is a modification of [40] work. Unlike the previous study, the current work divided humans, livestock and maize kernels into subgroups depending on the status of aflatoxins contamination. We use three controls: good

Table 1
Model variables.

Variable	Description	Units
$S_C(t)$	Susceptible maize kernels at time t	$Maizekernels$
$C_C(t)$	Contaminated maize kernels at time t	$Maizekernels$
$S_L(t)$	Susceptible livestock at time t	$Livestock$
$C_L(t)$	Contaminated livestock at time t	$Livestock$
$S_H(t)$	Susceptible humans at time t	$Humans$
$C_H(t)$	Contaminated humans at time t	$Humans$
$A(t)$	Aflatoxin fungi per unit volume in soil at time t	$Aflatoxinfungi$

farming practices, biological control and public education and awareness campaigns, instead of the one control used in the previous study. The current study also provides a cost-effective analysis of the suggested strategy to reduce the burden on farmers. The human population is divided into susceptible $S_H(t)$ and contaminated $C_H(t)$ subgroups, the livestock population is also divided into susceptible $S_L(t)$ and contaminated $C_L(t)$ subgroups and the maize kernels are divided into susceptible $S_C(t)$ and contaminated $C_C(t)$ subgroups. Another compartment is Aflatoxin fungi $A(t)$ which represent the amount of *Aspergillus flavus* and *Aspergillus parasiticus* per unit volume in environment at time t. We assume an average recruitment rate of aflatoxin fungi in environment without looking at all sources or stimuli for simplicity. Individuals in the susceptible group have not been contaminated by aflatoxin and thus they are aflatoxicosis free. In contaminated groups, individuals have been contaminated with aflatoxin.

Maize kernels are recruited at maize kernels' production rate of π_C. Aflatoxins are produced when susceptible maize kernels contact *Aspergillus flavus* and *Aspergillus parasiticus* fungi provided there are favorable conditions. Susceptible maize kernels are contaminated at a force of contamination function $\theta_1 = \beta_1 A$, where β_1 is the contamination rate of susceptible maize kernels from aflatoxins. Livestock are recruited at the rate of π_L through birth. Susceptible livestock acquire aflatoxin through consumption of contaminated feeds and become contaminated at a force of contamination function $\theta_2 = \beta_2 C_C$, where β_2 is the contamination rate of susceptible livestock from contaminated maize kernels. Susceptible humans acquire aflatoxin directly through consumption of contaminated food and indirectly through consumption of contaminated livestock products at a force of contamination function $\theta_3 = \beta_4 C_C + \beta_5 C_L$, where β_4 is the contamination rate of humans from contaminated maize kernels and β_5 is the contamination rate of humans from contaminated livestock products. Other ways of transmission have very minimal effects [19,50,51] in dynamics of contamination and therefore excluded in the current study.

We incorporate in the mathematical model for the transmission dynamics of aflatoxin contamination some time-dependent controls to some parameters. A time-dependent control variable $u_1(t)$ such that $0 \leq u_1(t) \leq 1$ represents good farming practices that aims to reduce contaminated maize kernels. It involves the use of resistant cultivars, crop rotation, weed and pest control. In other words, $u_1(t)$ measures the effectiveness of good farming practices while $(1-u_1(t))$ is the failure rate of good farming practices. Thus, if good farming practices are applied 100% then, zero aflatoxin contamination in maize kernels may be achieved. Another time-dependent control variable $u_2(t)$ such that $0 \leq u_2(t) \leq 1$ represent biological control that aims to reduce aflatoxin fungi in soil. It involves the use of atoxigenic fungi (non-aflatoxigenic) to competitively displace the toxigenic fungi (aflatoxigenic). Aflasafe is an example of non-aflatoxigenic fungi used to displace the aflatoxigenic fungi. We also introduce another parameter, $\sigma \in [0,1]$ which measure the effectiveness of biological control in reducing or eliminating aflatoxin fungi in soil. The last time-dependent control variable $u_3(t)$ such that $0 \leq u_3(t) \leq 1$ represents public education and awareness campaigns that aim to reduce aflatoxin contamination in livestock and humans. It should be noted that education and awareness campaigns are targeting human beings, but there are indirect effects on livestock since humans are the ones who feed them. Thus, $u_3(t)$ measures the effectiveness of public education and awareness campaigns while $(1-u_3(t))$ is the failure rate of public education and awareness campaigns on humans and consequently on livestock. Thus, if public education and awareness campaigns are 100% effective then, zero livestock and humans contamination my be achieved.

In formulating a mathematical model, we assumed the following:

(i) The environment is a reservoir of aflatoxin fungi and can be maintained for a prolonged period [52–54].
(ii) Contaminated maize kernels add aflatoxin fungi in soil [52,53].
(iii) Maize kernels are the only hosts for aflatoxin fungi. Without these hosts, aflatoxin fungi remain dormant in the soil [52,55,56].
(iv) Aflatoxin fungi intrude maize kernels from soil and form aflatoxin when there are favorable conditions [19,52,55,56].
(v) Susceptible livestock get aflatoxins through consuming contaminated maize kernels [11,19].
(vi) Susceptible humans get aflatoxins through consuming contaminated maize kernels, livestock or their contaminated products [11,19,50,51].
(vii) Once maize kernels, livestock and humans are contaminated with aflatoxin, the toxins cannot be removed completely [19,50,51].
(vii) All recruits in each population are susceptible to aflatoxin contaminations [11].

The variables and parameters used in model are explained in Table 1 and 2 respectively. Based on the dynamics of the aflatoxin contamination, model assumptions, definition of variables and parameters, the dynamics of aflatoxin contamination is summarized in the flow diagram as shown by Fig. 1.

Table 2
Description of the model parameters.

Parameter	Description	Unit
β_1	Aflatoxin contamination rate of maize kernels	$(A.fungi \times year)^{-1}$
β_2	Aflatoxin contamination rate of livestock from maize kernels	$(Maizekernels \times year)^{-1}$
β_4	Aflatoxin contamination rate of humans from maize kernels	$(Maizekernels \times year)^{-1}$
β_5	Aflatoxin contamination rate of humans from livestock	$(Livestock \times year)^{-1}$
ρ	Shading rate of aflatoxin fungi in soil from maize kernels	$Aflatoxinfungi(Maizekernels \times year)^{-1}$
π_C	maize kernels production rate	$maizekernels \times year^{-1}$
π_L	Recruitment rate of livestock	$Livestock \times year^{-1}$
π_H	Recruitment rate of humans	$Humans \times year^{-1}$
μ_L	Natural death rate of livestock	$year^{-1}$
μ_H	Natural death rate of humans	$year^{-1}$
ϕ_L	Livestock death rate due to aflatoxicosis	$year^{-1}$
ϕ_H	Human death rate due to aflatoxicosis	$year^{-1}$
ω_1	Consumption rate of maize kernels	$year^{-1}$
μ_C	Loss rate of maize kernels	$year^{-1}$
α	Reduction rate of aflatoxin fungi in soil	$year^{-1}$

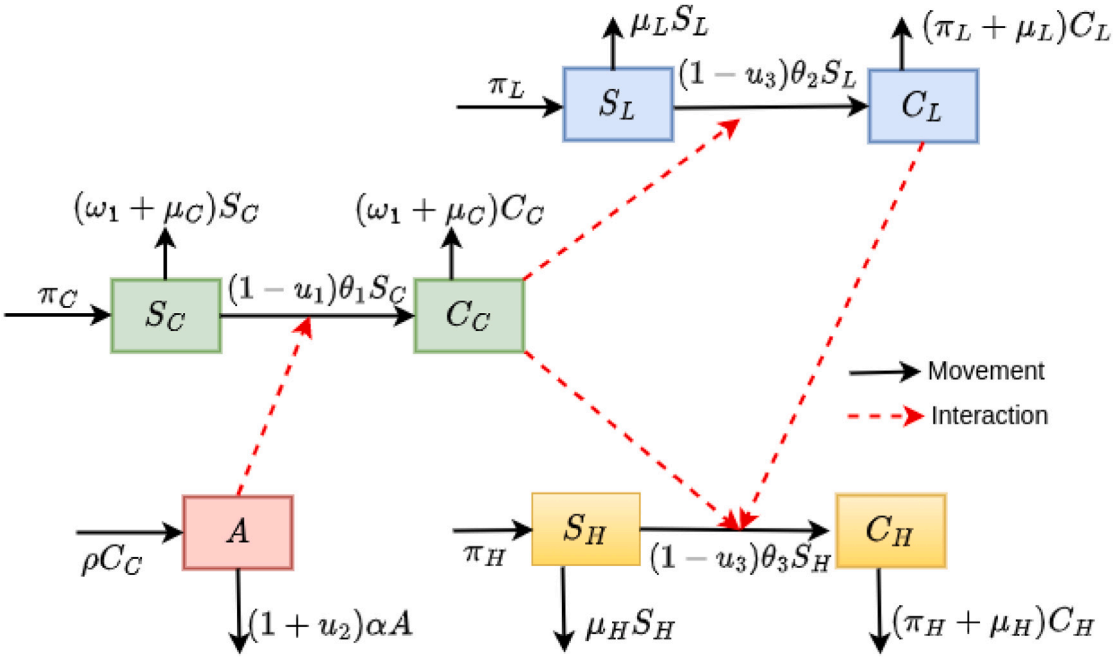

Fig. 1. Aflatoxin contamination dynamics compartmental flow diagram with control parameters.

The dynamics of aflatoxin contamination is summarized by the following differential equations:

$$\begin{cases} \frac{dS_C}{dt} &= \pi_C - ((1-u_1(t))\beta_1 A + \omega_1 + \mu_C)S_C, \\ \frac{dC_C}{dt} &= (1-u_1(t))\beta_1 A S_C - (\omega_1 + \mu_C)C_C, \\ \frac{dS_L}{dt} &= \pi_L - ((1-u_3(t))\beta_2 C_C + \mu_L)S_L, \\ \frac{dC_L}{dt} &= (1-u_3(t))\beta_2 C_C S_L - (\mu_L + \phi_L)C_L, \\ \frac{dS_H}{dt} &= \pi_H - ((1-u_3(t))(\beta_4 C_C + \beta_5 C_L) + \mu_H)S_H, \\ \frac{dC_H}{dt} &= (1-u_3(t))(\beta_4 C_C + \beta_5 C_L)S_H - (\mu_H + \phi_H)C_H, \\ \frac{dA}{dt} &= \rho C_C - (1+u_2)\alpha A, \end{cases} \tag{1}$$

subject to the following non-negative initial conditions

$$S_C(0) > 0, \quad C_C(0) \geq 0, \quad S_L(0) > 0, \quad C_L(0) \geq 0, \quad S_H(0) > 0, \quad C_H(0) \geq 0, \quad A(0) \geq 0. \tag{2}$$

3. Model analysis

In this section we perform the analysis of the model by considering both positivity of solutions and model boundedness. The equilibrium points and their stability are also discussed in this section.

3.1. Positivity of solutions

We demonstrate that the solution of model system (1) remain positive for all non-negative initial conditions in invariant region using the approach by [57–59].

Taking the first equation of system (1),

$$\frac{dS_C}{dt} = \pi_C - \beta_1 A S_C - \omega_1 S_C - \mu_C S_C.$$

Let $S_C(0) > 0$.

Now suppose that $\exists\ t = t_0 > 0$ such that $S_C(t_0) = 0$, $\frac{dS_C(t_0)}{dt} < 0$, $C_C(t_0) \geq 0$, $S_L(t_0) > 0$, $C_L(t_0) \geq 0$, $S_H(t_0) > 0$, $C_H(t_0) \geq 0$ and $A(t_0) \geq 0$..

Thus,

$$\frac{dS_C(t_0)}{dt} = \pi_C - \beta_1 A(t_0) S_C(t_0) - \omega_1 S_C(t_0) - \mu_C S_C(t_0) = \pi_C > 0.$$

Which is a contradiction. Therefore, $S_C(t) > 0\ \forall\ t$.

Taking the second equation of system (1),

$$\frac{dC_C}{dt} = \beta_1 A S_C - \omega_1 C_C - \mu_C C_C.$$

Let $C_C(0) \geq 0$.

Now suppose that $\exists\ t = t_1 > 0$ such that $C_C(t_1) = 0$, $\frac{dC_C(t_1)}{dt} < 0$, $S_C(t_1) > 0$, $S_L(t_1) > 0$, $C_L(t_1) \geq 0$, $S_H(t_1) > 0$, $C_H(t_1) \geq 0$ and $A(t_1) \geq 0$..

Thus,

$$\frac{dC_C(t_1)}{dt} = \beta_1 A(t_1) S_C(t_1) - \omega_1 C_C(t_1) - \mu_C C_C(t_1) \geq 0$$

Which is a contradiction. Therefore, $C_C(t) \geq 0\ \forall\ t$.

The positivity of all other variables in system (1) can be proved using the same approach. Therefore, we conclude that: $S_C > 0$, $C_C \geq 0$, $S_L > 0$, $C_L \geq 0$, $S_H > 0$, $C_H \geq 0$ and $A \geq 0$ for model system (1). The positivity of solution has the physical meaning that susceptible maize kernels, livestock and humans cannot be zero since they are recruited each year. However, contaminated maize kernels, livestock, humans and aflatoxin fungi can be zero when there is no contamination in populations.

3.2. Boundedness of the system

Model system (1) can be divided into the following independent sub-systems:

$$\begin{cases} \frac{dS_C}{dt} &= \pi_C - (1-u_1)\beta_1 A S_C - \omega_1 S_C - \mu_C S_C, \\ \frac{dC_C}{dt} &= (1-u_1)\beta_1 A S_C - \omega_1 C_C - \mu_C C_C. \end{cases} \tag{3}$$

$$\begin{cases} \frac{dS_L}{dt} &= \pi_L - (1-u_3)\beta_2 C_C S_L - \mu_L S_L, \\ \frac{dC_L}{dt} &= (1-u_3)\beta_2 C_C S_L - (\mu_L + \phi_L) C_L. \end{cases} \tag{4}$$

$$\begin{cases} \frac{dS_H}{dt} &= \pi_H - (1-u_3)\beta_4 C_C S_H - \beta_5 C_L S_H - \mu_H S_H, \\ \frac{dC_H}{dt} &= (1-u_3)\beta_4 C_C S_H + \beta_5 C_L S_H - (\mu_H + \phi_H) C_H. \end{cases} \tag{5}$$

From systems 3.2, and it can be shown that

$$\frac{d(S_C + C_C)}{dt} = \pi_C - (\omega_1 + \mu_C) S_C - (\omega_1 + \mu_C) C_C \leq \pi_C - (\omega_1 + \mu_C) S_C,$$

$$\frac{d(S_L + C_L)}{dt} = \pi_L - \mu_L S_L - (\mu_L + \phi_L) C_L \leq \pi_L - \mu_L S_L,$$

$$\frac{d(S_H + C_H)}{dt} = \pi_H - \mu_H S_H - (\mu_H + \phi_H)C_H \leq \pi_H - \mu_H S_H,$$

It follows that $\lim_{t\to\infty} sup(S_C + C_C) \leq \frac{\pi_C}{\omega_1 + \mu_C}$, $\lim_{t\to\infty} sup(S_L + C_L) \leq \frac{\pi_L}{\mu_L}$ and $\lim_{t\to\infty} sup(S_H + C_H) \leq \frac{\pi_C}{\mu_H}$.

Considering the last equation of model system (1) for aflatoxin fungi in the environment, we have:

$$\frac{dA}{dt} = \rho C_C - (1 + u_2)\alpha A$$

Since the total amount of maize kernels $S_C + C_C \leq \pi_C/(\omega_1 + \mu_C)$, it can be concluded that $C_C \leq \pi_C/(\omega_1 + \mu_C)$.

Thus,

$$\frac{dA}{dt} \leq \frac{\rho\pi_C}{\omega_1 + \mu_C} - (1 + u_2)\alpha A.$$

It follows that,

$$\lim_{t\to\infty} sup(A) \leq \frac{\rho\pi_C}{(1 + u_2)\alpha(\omega_1 + \mu_C)}$$

So, it can be concluded that the set

$$\Omega = \left\{ (S_C, C_C, S_L, C_L, S_H, C_H, A) \in \mathbb{R}^7_+ | 0 \leq S_C + C_C \leq \frac{\pi_C}{\omega_1 + \mu_C}, 0 \leq S_L + C_L \leq \frac{\pi_L}{\mu_L}, \right.$$
$$\left. 0 \leq S_H + C_H \leq \frac{\pi_C}{\mu_H}, 0 \leq A \leq \frac{\rho\pi_C}{(1 + u_2)\alpha(\omega_1 + \mu_C)} \right\}$$

is bounded with respect to model system (1). Therefore, Ω is a feasible region for model system (1).

3.3. Aflatoxin contamination free equilibrium (CFE) point

We consider system (1) where $u_1(t)$, $u_2(t)$ and $u_3(t)$ are time dependent controls. To obtain an aflatoxin contamination-free equilibrium point, the right side of equations in model system (1) is set to zero. All forces of contamination are also set to zero; $C_C = C_L = C_H = A = 0$. The aflatoxin contamination-free equilibrium point denoted by E^0 and is given by

$$E^0(S_C^0, C_C^0, S_L^0, C_L^0, S_H^0, C_H^0, A^0) = \left[\frac{\pi_C}{\omega_1 + \mu_C}, 0, \frac{\pi_L}{\mu_L}, 0, \frac{\pi_H}{\mu_H}, 0, 0 \right].$$

3.3.1. Effective aflatoxin contamination number

We calculate the effective aflatoxin contamination number using next generation matrix [60,61]. Consider system 3.3.1 of contaminated variables

$$\begin{cases} \frac{dC_C}{dt} &= (1 - u_1)\beta_1 A S_C - (\omega_1 + \mu_C)C_C, \\ \frac{dC_L}{dt} &= (1 - u_3)\beta_2 C_C S_L - (\mu_L + \phi_L)C_L, \\ \frac{dC_H}{dt} &= (1 - u_3)\beta_4 C_C S_H + (1 - u_3)\beta_5 C_L S_H - (\mu_H + \phi_H)C_H, \\ \frac{dA}{dt} &= \rho C_C - (1 + u_2)\alpha A. \end{cases} \tag{6}$$

The effective contamination number is obtained by finding the spectral radius of the next generation matrix

$$FV^{-1} = \left[\frac{\partial \mathcal{F}_i(E^0)}{\partial t} \right] \left[\frac{\partial \mathcal{V}_i(E^0)}{\partial t} \right]^{-1}$$

where E^0 is an aflatoxin contamination free equilibrium point, the vector $\mathcal{F}_i$ refers to new aflatoxin contamination appearance rate in compartment i while vector $\mathcal{V}_i$ is the transfer of contamination out of compartment i, such that

$$\mathcal{F}_i = \begin{bmatrix} (1 - u_1)\beta_1 A S_C \\ (1 - u_3)\beta_2 C_C S_L \\ (1 - u_3)\beta_4 C_C S_H + (1 - u_3)\beta_5 C_L S_H \\ 0 \end{bmatrix}, \quad \mathcal{V}_i = \begin{bmatrix} (\omega_1 + \mu_C)C_C \\ (\mu_L + \phi_L)C_L \\ (\mu_H + \phi_H)C_H \\ -\rho C_C + (1 + u_2)\alpha A. \end{bmatrix},$$

The Jacobian matrices of $\mathcal{F}_i$ and $\mathcal{V}_i$ at E^0, the variational matrices F and V are obtained respectively as

$$F = \begin{bmatrix} 0 & 0 & 0 & \frac{(1-u_1)\beta_1\pi_C}{\omega_1+\mu_C} \\ \frac{(1-u_3)\beta_2\pi_L}{\mu_L} & 0 & 0 & 0 \\ \frac{(1-u_3)\beta_4\pi_H}{\mu_H} & \frac{(1-u_3)\beta_5\pi_H}{\mu_H} & 0 & 0 \\ 0 & 0 & 0 & 0 \end{bmatrix}, \tag{7}$$

$$V = \begin{bmatrix} \omega_1+\mu_C & 0 & 0 & 0 \\ 0 & \phi_L+\mu_L & 0 & 0 \\ 0 & 0 & \phi_H+\mu_H & 0 \\ -\rho & 0 & 0 & (1+u_2)\alpha \end{bmatrix}. \tag{8}$$

The inverse of variational matrix V becomes

$$V^{-1} = \begin{bmatrix} \frac{1}{\omega_1+\mu_C} & 0 & 0 & 0 \\ 0 & \frac{1}{\phi_L+\mu_L} & 0 & 0 \\ 0 & 0 & \frac{1}{\phi_H+\mu_H} & 0 \\ \frac{\rho}{(\omega_1+\mu_C)(\alpha u_2+\alpha)} & 0 & 0 & \frac{1}{\alpha u_2+\alpha} \end{bmatrix}.$$

The next generation matrix is obtained as

$$FV^{-1} = \begin{bmatrix} \frac{(1-u_1)\beta_1\pi_c\rho}{(\omega_1+\mu_C)^2(\alpha u_2+\alpha)} & 0 & 0 & \frac{(1-u_1)\beta_1\pi_c}{(\omega_1+\mu_C)(\alpha u_2+\alpha)} \\ \frac{(1-u_3)\beta_2\pi_L}{\mu_L(\omega_1+\mu_C)} & 0 & 0 & 0 \\ \frac{(1-u_3)\beta_4\pi_H}{\mu_H(\omega_1+\mu_C)} & \frac{(1-u_3)\beta_5\pi_H}{\mu_H(\phi_L+\mu_L)} & 0 & 0 \\ 0 & 0 & 0 & 0 \end{bmatrix}. \tag{9}$$

The effective contamination number, R_e is obtained by computing the spectral radius $\left(FV^{-1}\right)$ of the next generation matrix. Thus, the dominant eigenvalue of matrix (9) gives the effective contamination number as;

$$\text{Spectral radius of } FV^{-1} = R_e = \frac{\rho\beta_1\pi_C(1-u_1)}{(\omega_1+\mu_C)^2(1+u_2)\alpha} \tag{10}$$

It can be seen that

$$R_e = R_{eA} \cdot R_{eC} \tag{11}$$

where

$$R_{eA} = (1-u_1)\beta_1 S_C^0 \cdot \frac{1}{\omega_1+\mu_C},$$

$$R_{eC} = \rho \cdot \frac{1}{\alpha(1+u_2)}.$$

The effective contamination number, R_e is analogous to effective reproduction number in epidemiological models, a threshold quantity used to examine equilibrium points. It is a crucial quantity that defines how contamination behaves. If $R_e > 1$, aflatoxin contamination persists and if $R_e < 1$, aflatoxin contamination diminishes. On R_{eA}, the term $(1-u_1)\beta_1 S_C^0$ represent new contamination under control while $\frac{1}{\omega_1+\mu_C}$ represent duration of aflatoxin contamination stay in contaminated maize kernels. On R_{eC}, the term ρ represent new aflatoxin fungi in soil from maize kernels while $\frac{1}{\alpha(1+u_2)}$ represent duration of stay of aflatoxin fungi in soil under control. In this case, R_e is defined as number of tonnes of contaminated maize kernels as a result of one tonne of contaminated maize kernels. When there is no control for aflatoxin contamination ($u_1 = u_2 = 0$), the effective contamination number reduces to basic contamination number given by Eq. (12).

$$R_0 = \frac{\rho\beta_1\pi_C}{(\omega_1+\mu_C)^2\alpha} \tag{12}$$

Also, R_0 can be broken into

$$R_0 = R_{0A} \cdot R_{0C} \tag{13}$$

where

$$R_{0A} = \beta_1 S_C^0 \cdot \frac{1}{\omega_1 + \mu_C},$$

$$R_{0C} = \rho \cdot \frac{1}{\alpha}.$$

The terms in R_{0A} and R_{0C} have same interpretation as in R_{eA} and R_{eC} when there are no controls.

Theorem 1 follows from Theorem 2 of [61].

Theorem 1. *The aflatoxin contamination-free equilibrium point of model system (1) is locally asymptotically stable if $R_e < 1$ and unstable if $R_e > 1$.*

3.3.2. Global stability of aflatoxin contamination free equilibrium point

In this subsection we perform global stability analysis of aflatoxin contamination free equilibrium point using the approach explained by [62]. Model system (1) can be expressed as:

$$\begin{cases} \dfrac{dX_S}{dt} = A(X_S - X_{DFE,S}) + A_1 X_C, \\ \dfrac{dX_C}{dt} = A_2 X_C, \end{cases}$$

where, X_S is the vector representing the compartments that do not transmit aflatoxin and X_C represent aflatoxin contaminating compartments. In case A_2 is a stable Metzler matrix and A has real negative eigenvalues, the aflatoxin contamination free equilibrium is globally asymptotically stable. From the model system (1) it can be deduced that:

$$X_C = (C_C, C_L, C_H, A)^T, \quad X_S = (S_C, S_L, S_H)^T,$$

$$X_S - X_{DFE,S} = \begin{bmatrix} S_C - \dfrac{\pi_C}{\omega_1 + \mu_C} \\ S_L - \dfrac{\pi_L}{\mu_L} \\ S_H - \dfrac{\pi_H}{\mu_H} \end{bmatrix}, \quad A_1 = \begin{bmatrix} 0 & 0 & 0 & -(1-u_1)\beta_1 S_C \\ -(1-u_3)\beta_2 S_L & 0 & 0 & 0 \\ -(1-u_3)\beta_4 S_H & -(1-u_3)\beta_5 S_H & 0 & 0 \end{bmatrix}.,$$

Matrix A is obtained from non contaminating classes in system (1) and is given by:

$$A = \begin{bmatrix} -(\omega_1 + \mu_C) & 0 & 0 \\ 0 & -\mu_L & 0 \\ 0 & 0 & -\mu_H \end{bmatrix}.$$

It can be seen that the eigenvalues of matrix A are all negative; $\lambda_1 = -\omega_1 - \mu_C$, $\lambda_2 = -\mu_L$ and $\lambda_3 = -\mu_H$.

Matrix A_2 is obtained from contaminating classes in system (1) and is given by:

$$A_2 = \begin{bmatrix} -(\omega_1 + \mu_C) & 0 & 0 & \dfrac{(1-u_1)\beta_1 \pi_C}{\omega_1 + \mu_C} \\ \dfrac{(1-u_3)\beta_2 \pi_L}{\mu_L} & -(\mu_L + \phi_L) & 0 & 0 \\ \dfrac{(1-u_3)\beta_4 \pi_H}{\mu_H} & \dfrac{(1-u_3)\beta_5 \pi_H}{\mu_H} & -(\mu_H + \phi_H) & 0 \\ \rho & 0 & 0 & -(1+u_2)\alpha \end{bmatrix}.$$

It can be observed that matrix A_2 is the Metzler matrix since its out-diagonal entries are non-negative. To prove the stability of A_2, we adopt the idea of stable Metzler matrix [63] and apply Lemma 2.

Lemma 2. *Let M be a square Metzler matrix written in block form:*

$$M = \begin{bmatrix} U & V \\ X & Y \end{bmatrix}$$

where U and Y are square matrices. M is Metzler stable if and only if matrices U and $Y - XU^{-1}V$ are Metzler stable [64,65].

Proof. Comparing Metzler matrix A_2 with a Metzler matrix M, matrices U, V, X and Y are obtained as:

$$U = \begin{bmatrix} -(\omega_1+\mu_C) & 0 \\ \dfrac{(1-u_3)\beta_2\pi_L}{\mu_L} & -(\mu_L+\phi_L) \end{bmatrix}, \quad V = \begin{bmatrix} 0 & \dfrac{(1-u_1)\beta_1\pi_C}{\omega_1+\mu_C} \\ 0 & 0 \end{bmatrix}$$

$$X = \begin{bmatrix} \dfrac{(1-u_3)\beta_4\pi_H}{\mu_H} & \dfrac{(1-u_3)\beta_5\pi_H}{\mu_H} \\ \rho & 0 \end{bmatrix}, \quad Y = \begin{bmatrix} -(\mu_H+\phi_H) & 0 \\ 0 & -(1+u_2)\alpha \end{bmatrix},$$

It can be seen clearly that matrix U is stable matrix since all eigenvalues have negative real parts. Up on computation we obtain:

$$Y - XU^{-1}V = \begin{bmatrix} -(\mu_H+\phi_H) & \dfrac{\pi_H\left((1-u_3)^2\beta_5\beta_2\pi_L + (1-u_2)\beta_4{\mu_L}^2 + (1-u_2)\beta_4\mu_L\phi_L\right)\beta_1\pi_C}{\mu_H\mu_L\left(\omega_1+\mu_C\right)^2\left(\mu_L+\phi_L\right)} \\ 0 & -(1-R_e)(1+u_2)\alpha \end{bmatrix}$$

$Y - XU^{-1}V$ is Metzler stable if $R_e < 1$. Therefore, the aflatoxin contamination free equilibrium point of the model system (1) is globally asymptotically stable if $R_e < 1$. The global asymptotic stability of aflatoxin contamination free equilibrium point implies that if the system starts in any initial conditions the dynamics of the system will converge and eventually lead to the eradication of the contamination, and the populations will reach and stay in the contamination-free state. This property is important as it indicates the possibility of eliminating contamination from a populations and maintaining long-term contamination control. However, if controls are not reducing R_e below unit, aflatoxin contamination will persist. Also, there is possibility of chemical aflatoxin resistance due to chemical controls and development of other types of contamination due to biological controls. □

3.4. Aflatoxin contamination persistence equilibrium (ACPE) point

The aflatoxin contamination persistence equilibrium point $E^*\left(S_C^*, C_C^*, S_L^*, C_L^*, S_H^*, S_H^*, A^*\right)$ of the model system (1) is obtained by setting all equations to zero and solving for the state variables. After solving E^* is given by:

$$S_C^* = \frac{\pi_C}{R_e\left(\omega_1+\mu_C\right)}$$

$$C_C^* = \frac{Q_7(R_e-1)}{Q_8}$$

$$S_L^* = \frac{Q_1R_e^2}{Q_2(R_e-1)+Q_3R_e}$$

$$C_L^* = \frac{Q_4R_e(R_e-1)}{Q_5(R_e-1)+Q_6R_e}$$

$$S_H^* = \frac{\pi_HQ_8\left(Q_5\left(R_e-1\right)+Q_6R_e\right)}{\beta_4\left(Q_5\left(R_e-1\right)+Q_6R_e\right)Q_7\left(R_e-1\right)-Q_8\left(Q_9+Q_4R_e\left(R_e-1\right)\beta_5+\mu_HQ_5\left(R_e-1\right)\right)}$$

$$C_H^* = \frac{\left(\beta_4\left(Q_5\left(R_e-1\right)+Q_6R_e\right)Q_7\left(R_e-1\right)+Q_4R_e\left(R_e-1\right)\beta_5Q_8\right)\pi_H}{\left(\beta_4\left(Q_5\left(R_e-1\right)+Q_6R_e\right)Q_7\left(R_e-1\right)-Q_8\left(Q_9+Q_4R_e\left(R_e-1\right)\beta_5+\mu_HQ_5\left(R_e-1\right)\right)\right)Q_{10}}$$

$$A^* = \left(R_e-1\right)\left(\omega_1+\mu_C\right)$$

The denominator of S_H^* can be simplified to

$$\left[\beta_4Q_6Q_7+Q_5Q_7-Q_4Q_5Q_8\right](R_e-1)^2+\left[\beta_4Q_6Q_7-Q_5Q_8\mu_H\right](R_e-1)-Q_8(Q_4+Q_9)$$

Using completing the square technique we obtain the following:

$$\left[(R_e-1)-\frac{Q_{13}+Q_5Q_7-Q_{14}}{Q_{13}-Q_5Q_8\mu_H}\right]^2-\frac{4\left[Q_{13}+Q_5Q_7-Q_{14}\right](Q_8(Q_4+Q_9))}{4\left[Q_{13}+Q_5Q_7-Q_{14}\right]^2}-\frac{(Q_{13}-Q_5Q_8\mu_H)^2}{4\left[Q_{13}+Q_5Q_7-Q_{14}\right]^2}$$

Upon simplification we have:

$$\left[(R_e-1)-\frac{Q_{13}+Q_5Q_7-Q_{14}}{Q_{13}-Q_5Q_8\mu_H}\right]^2+\frac{Q_8(Q_4+Q_9)}{Q_{12}\left[(1+Q_{11})+(R_e-1)Q_{11}\right]}+\frac{\left[Q_{13}-Q_5Q_8\mu_H\right]^2}{4\left[Q_{13}+Q_5Q_7-Q_{14}\right]^2}$$

Similarly, the denominator of C_H^* can be simplified to

$$\left[(R_e-1)-\frac{Q_{13}+Q_5Q_7-Q_{14}}{Q_{13}-Q_5Q_8\mu_H}\right]^2Q_{10}+\frac{Q_8(Q_4+Q_9)Q_{10}}{Q_{12}\left[(1+Q_{11})+(R_e-1)Q_{11}\right]}+\frac{\left[Q_{13}-Q_5Q_8\mu_H\right]^2Q_{10}}{4\left[Q_{13}+Q_5Q_7-Q_{14}\right]^2}$$

where $Q_1 = (\omega_1+\mu_C)^3(1+u_2)\alpha\pi_L$, $Q_2 = \pi_C^2\rho\beta_1(1-u_1)\beta_2(1-u_3)$, $Q_3 = \pi_C\rho\beta_1(1-u_1)(\mu_C\mu_L+\mu_L\omega_1)$, $Q_4 = (1+u_2)\alpha(\omega_1+\mu_C)^2$, $Q_5 = \pi_C\rho\beta_1(1-u_1)\beta_2(1-u_3)(\phi_L+\mu_L)$, $Q_6 = \rho\beta_1(1-u_1)(\phi_L+\mu_L)(\mu_C\mu_L+\mu_L\omega_1)$, $Q_7 = (1+u_2)\alpha(\omega_1+\mu_C)$, $Q_8 = \rho\beta_1(1-u_1)$, $Q_9 = R_eQ_6\mu_H$, $Q_{10} = (\mu_H+\phi_H)$, $Q_{11} = \dfrac{(\omega_1+\mu_C)^2(1+u_2)\alpha}{\pi_C}$, $Q_{12} = Q_5(1+u_2)\alpha(\omega_1+\mu_C)$, $Q_{13} = \beta_4Q_6Q_7$ and $Q_{14} = Q_4Q_5Q_8$.

Therefore, the aflatoxin contamination persistence equilibrium point exist if $R_e > 1$.

3.4.1. Global stability of aflatoxin contamination persistence equilibrium point

Theorem 3. *The aflatoxin contamination persistence equilibrium point of the aflatoxin contamination model system (1) is globally asymptotically stable on Ω if $R_e > 1$.*

Proof. We use a Lyapunov function of model system (1) as describe by [66,67] and used by [68,69]. The Lyapunov function H is defined by

$$H = \sum P_i\left(y_i - y_i^* - y_i^*\ln\frac{y_i}{y_i^*}\right)$$

where P_i denotes a positive constant to be determined, y_i denotes a population of ith compartment and y_i^* denotes an aflatoxin contamination persistence equilibrium point of the model. It is clear that the function H satisfy all condition for Lyapunov function as follows:

(i) H is zero at the equilibrium $E^*\left(S_C^*, C_C^*, S_L^*, C_L^*, S_H^*, S_H^*, A^*\right)$
(ii) H is positive for all other values of $S_C, C_C, S_L, C_L, S_H, S_H$ and A.

A Lyapunov function H of the model system (10) is defined by

$$\begin{aligned} H =& P_1(S_C - S_C^* - S_C^*\ln\frac{S_C}{S_C^*}) + P_2(C_C - C_C^* - C_C^*\ln\frac{C_C}{C_C^*}) + P_3(S_L - S_L^* - S_L^*\ln\frac{S_L}{S_L^*}) \\ &+ P_4(C_L - C_L^* - C_L^*\ln\frac{C_L}{C_L^*}) + P_5(S_H - S_H^* - S_H^*\ln\frac{S_H}{S_H^*}) + P_6(C_H - C_H^* - C_H^*\ln\frac{C_H}{C_H^*}) \\ &+ P_7(A - A^* - A^*\ln\frac{A}{A^*}). \end{aligned} \tag{14}$$

where $P_1, P_2, P_3, P_4, P_5, P_6$ and P_7 are positive constants to be determined. The derivative of the Lyapunov function H with respect to time is given by

$$\begin{aligned} \frac{dH}{dt} =& P_1\left(1-\frac{S_C^*}{S_C}\right)\frac{dS_C}{dt} + P_2\left(1-\frac{C_C^*}{C_C}\right)\frac{dC_C}{dt} + P_3\left(1-\frac{S_L^*}{S_L}\right)\frac{dS_L}{dt} + P_4\left(1-\frac{C_L^*}{C_L}\right)\frac{dC_L}{dt} \\ &+ P_5\left(1-\frac{S_H^*}{S_H}\right)\frac{dS_H}{dt} + P_6\left(1-\frac{C_H^*}{C_H}\right)\frac{dC_H}{dt} + P_7\left(1-\frac{A^*}{A}\right)\frac{A}{dt}. \end{aligned} \tag{15}$$

Substituting $\frac{dS_C}{dt}$, $\frac{dC_C}{dt}$, $\frac{dS_L}{dt}$, $\frac{dC_L}{dt}$, $\frac{dH_H}{dt}$, $\frac{dC_H}{dt}$ and $\frac{dA}{dt}$ in Eq. (15) it yields

$$\begin{aligned} \frac{dH}{dt} =& P_1\left(1-\frac{S_C^*}{S_C}\right)\left[\pi_C - z_1\beta_1AS_C - k_1S_C\right] \\ &+ P_2\left(1-\frac{C_C^*}{C_C}\right)\left[z_1\beta_1AS_C - k_1C_C\right] \\ &+ P_3\left(1-\frac{S_L^*}{S_L}\right)\left[\pi_L - z_3\beta_2C_CS_L - \mu_LS_L\right] \\ &+ P_4\left(1-\frac{C_L^*}{C_L}\right)\left[z_3\beta_2C_CS_L - k_2C_L\right] \\ &+ P_5\left(1-\frac{S_H^*}{S_H}\right)\left[\pi_H - z_3\beta_4C_CS_H - z_3\beta_5C_LS_H - \mu_HS_H\right] \\ &+ P_6\left(1-\frac{C_H^*}{C_H}\right)\left[z_3\beta_4C_CS_H + z_3\beta_5C_LS_H - k_3C_H\right] \\ &+ P_7\left(1-\frac{A^*}{A}\right)\left[\rho C_C - z_2\alpha A\right], \end{aligned} \tag{16}$$

where $k_1 = \omega_1+\mu_C$, $k_2 = \mu_L+\phi_L$, $k_3 = \mu_H+\phi_H$, $z_1 = 1-u_1$, $z_2 = 1+u_2$ and $z_3 = 1-u_3$.

At aflatoxin contamination persistence equilibrium point E^* Eq. (16) yields:

$$\begin{aligned} \frac{dH}{dt} =& P_1\left(1-\frac{S_C^*}{S_C}\right)\left[z_1\beta_1AS_C^* + k_1S_C^* - z_1\beta_1AS_C - k_1S_C\right] \\ &+ P_2\left(1-\frac{C_C^*}{C_C}\right)\left[z_1\beta_1AS_C - \frac{z_1\beta_1A^*S_C^*C_C}{C_C^*}\right] \end{aligned}$$

$$
\begin{aligned}
&+ P_3\left(1-\frac{S_L^*}{S_L}\right)\left[z_3\beta_2 C_C S_L^* + \mu_L S_L^* - z_3\beta_2 C_C S_L - \mu_L S_L\right] \\
&+ P_4\left(1-\frac{C_L^*}{C_L}\right)\left[z_3\beta_2 C_C S_L - \frac{z_3\beta_2 C_C^* S_L^* C_L}{C_L^*}\right] \\
&+ P_5\left(1-\frac{S_H^*}{S_H}\right)\left[z_3\beta_4 C_C^* S_H^* + z_3\beta_5 C_L^* S_H^* + \mu_H S_H^* - z_3\beta_4 C_C S_H - z_3\beta_5 C_L S_H - \mu_H S_H\right] \\
&+ P_6\left(1-\frac{C_H^*}{C_H}\right)\left[z_3\beta_4 C_C S_H + z_3\beta_5 C_L S_H - \frac{z_3\beta_4 C_C^* S_H^* C_H}{C_H^*} - \frac{z_3\beta_5 C_L^* S_H^* C_H}{C_H\,*}\right] \\
&+ P_7\left(1-\frac{A^*}{A}\right)\left[z_2\alpha A^* - \rho C_C^* + \rho C_C - z_2\alpha A\right].
\end{aligned} \tag{17}
$$

For simplification, let $e=\frac{S_C}{S_C^*}$, $f=\frac{C_C}{C_C^*}$, $g=\frac{S_L}{S_L^*}$, $h=\frac{C_L}{C_L^*}$, $m=\frac{S_H}{S_H^*}$, $n=\frac{C_H}{C_H^*}$ and $q=\frac{A}{A^*}$. Upon simplification, Eq. (17) yields;

$$
\begin{aligned}
\frac{dH}{dt} =& -P_1k_1S_C\left(1-\frac{1}{e}\right)^2 - P_3\mu_L S_L\left(1-\frac{1}{g}\right)^2 - P_5\mu_H S_H\left(1-\frac{1}{m}\right)^2 - P_7z_2\alpha A\left(1-\frac{1}{q}\right)^2 \\
&+ (P_1+P_2)z_1\beta_1A^*S_C^* + (P_3+P_4)z_3\beta_2C_C * S_L * + (P_5+P_6)\left[z_3\beta_4C_C^*S_H^* + z_3\beta_5C_L^*S_H^*\right] - P_7\rho C_C^* \\
&- P_1z_1\beta_1A^*S_C^*\cdot\frac{1}{e} + z_1\beta_1A^*S_C^*(P_2-P_1)\cdot eq + P_1z_1\beta_1A^*S_C^*\cdot q \\
&+ \left(P_3z_3\beta_2C_C * S_C^* + P_7\rho C_C^* - P_2z_1\beta_1A^*S_C^* + P_5z_3\beta_4C_C^*S_H^*\right)\cdot f - P_2z_1\beta_1A^*S_C^*\cdot\frac{eq}{f} \\
&+ z_3\beta_2C_C^*S_L^*(P_4-P_3)\cdot fg - P_3z_3\beta_2C_C^*S_L^*\cdot\frac{1}{g} + \left(P_5z_3\beta_5C_LS_H^* - P_4z_3\beta_2C_C^*S_L^*\right)\cdot h \\
&- P_4z_3\beta_2C_C^*S_L^*\cdot\frac{fg}{h} + (P_6-P_5)z_3\beta_4C_C^*S_H^*\cdot fm + (P_6-P_5)z_3\beta_4C_L^*S_H^*\cdot hm \\
&- P_5\left(z_3\beta_4C_C^*S_H^* + z_3\beta_5C_L^*S_H^*\right)\cdot\frac{1}{m} - P_6\left(z_3\beta_4C_C^*S_H^* + z_3\beta_5C_L^*S_H^*\right)\cdot n - P_6z_3\beta_4C_C^*S_H^*\cdot\frac{fm}{n} \\
&- P_6z_3\beta_5C_L^*S_H^*\cdot\frac{hm}{n} - P_7\rho C_C^*\cdot\frac{f}{q} + P_7\rho C_C^*\cdot\frac{1}{q}
\end{aligned} \tag{18}
$$

Setting the coefficients of eq, fg, h, fm and hm be equal to zero, we have $P_1=P_2=P_3=P_4=P_7=1$ and $P_5=P_6=\frac{\beta_2C_C^*S_L^*}{\beta_5C_L^*S_H^*}$. Eq. (18) can be written as;

$$
\begin{aligned}
\frac{dH}{dt} =& -P_1k_1S_C\left(1-\frac{1}{e}\right)^2 - P_3\mu_LS_L\left(1-\frac{1}{g}\right)^2 - P_5\mu_HS_H\left(1-\frac{1}{m}\right)^2 - P_7z_2\alpha A\left(1-\frac{1}{q}\right)^2 \\
&+ z_1\beta_1A^*S_C^*\left(2-\frac{1}{e}+q-f-\frac{eq}{f}\right) + z_3\beta_2C_C^*S_L^*\left(4+f-\frac{1}{g}-\frac{fg}{h}-\frac{1}{m}-n-\frac{hm}{n}\right) \\
&\frac{z_3\beta_2\beta_4C_C^*S_L^*}{\beta_5C_L^*}\left(2+f-\frac{1}{m}-n-\frac{fm}{n}\right) + \rho C_C^*\left(f-1-\frac{f}{q}+\frac{1}{q}\right)
\end{aligned} \tag{19}
$$

Consider a function $z(x)=1-x+\ln(x)\le 0$ for any $x>0$ with equality holds if $x=1$. Thus $1-x\le-\ln(x)$.

Taking:

$$
\begin{aligned}
2-\frac{1}{e}+q-f-\frac{eq}{f} &= \left(1-\frac{1}{e}\right)+(1-f)+\left(1-\frac{eq}{f}\right)-(1-q) \\
&\le -\ln(\frac{1}{e}) - \ln(f) - \ln\left(\frac{eq}{f}\right) + \ln(f) = \ln(e\cdot\frac{1}{f}\cdot\frac{f}{eq}\cdot q) = 0.
\end{aligned}
$$

$$
\begin{aligned}
4+f-\frac{1}{g}-\frac{fg}{h}-\frac{1}{m}-n-\frac{hm}{n} &= \left(1-\frac{1}{g}\right)+\left(1-\frac{fg}{h}\right)+\left(1-\frac{1}{m}\right)+(1-n)+\left(1-\frac{hm}{n}\right)-(1-f) \\
&\le -\ln\left(\frac{1}{g}\right) - \ln\left(\frac{fg}{h}\right) - \ln\frac{1}{m} - \ln(m) - \ln\left(\frac{hm}{n}\right) + \ln(f) \\
&= \ln\left(g\cdot\frac{h}{fg}\cdot m\cdot\frac{1}{n}\cdot\frac{n}{hm}\cdot f\right) = 0.
\end{aligned}
$$

$$
\begin{aligned}
2+f-\frac{1}{m}-n-\frac{fm}{n} &= \left(1-\frac{1}{m}\right)+(1-n)+\left(1-\frac{fm}{n}\right)-(1-f) \\
&\le -\ln\left(\frac{1}{m}\right) - \ln(n) - \ln\left(\frac{fm}{n}\right) + \ln(f) = \ln\left(m\cdot\frac{1}{n}\cdot\frac{n}{fm}\cdot f\right) = 0.
\end{aligned}
$$

$$
f-1-\frac{f}{q}+\frac{1}{q} = -(1-f)+\left(1-\frac{f}{q}\right)-\left(1-\frac{1}{q}\right)
$$

$$\leq \ln(f) - \ln\left(\frac{f}{g} + \ln\left(\frac{1}{q}\right)\right) = \ln\left(f \cdot \frac{q}{f} \cdot \frac{1}{q}\right) = 0$$

Thus, $\frac{dH}{dt} \leq 0$. Using LaSalle's extension to Lyapunov's method, the limit set of each solution is contained in the largest invariant set for which $S_C^* = S_C$, $C_C^* = C_C$, $S_L^* = S_L$, $C_L^* = C_L$, $S_H^* = S_H$, $C_H^* = C_H$, $A^* = A$ which is the singleton $\{E^*\}$ [70–72]. Hence, the aflatoxin contamination persistence equilibrium point (E^*) of the model system (1) is global asymptotically stable on Ω when $R_e > 1$. The global asymptotic stability of aflatoxin contamination persistence equilibrium point suggests that contamination will persist at a relatively constant level in the population, without dying out or causing a large-scale aflatoxin contamination. □

4. Optimal control problem

4.1. Formulation of the optimal control problem

The control theory is applied for the aim of minimizing the spread of aflatoxin contamination in maize kernels, livestock and humans. The purpose of introducing controls in the model is to find the optimal level of the intervention strategy preferred to reduce the aflatoxin contamination and cost of implementation of the control. The control variables $u_1(t)$, $u_2(t)$ and $u_3(t)$ are minimized subject to the differential Eqs. (1) and the minimization objective function presented as

$$J = \int_0^{t_f} \left(A_1 C_C + A_2 C_L + A_3 A + A_4 C_H + \frac{C_1 u_1^2}{2} + \frac{C_2 u_2^2}{2} + \frac{C_3 u_3^2}{2} \right) dt \tag{20}$$

where, A_1, A_2, A_3, and A_4, are positive constant weights representing cost for minimizing contaminated maize kernels, contaminated livestock, aflatoxin fungi and contaminated humans respectively. The coefficients C_1, C_2, and C_3 are relative cost weights for each individual control measure over a time period (t_f) for applying the control strategy. We use quadratic objective function (20), because a quadratic function is convex and smooth, making it easy to evaluate its derivative. Moreover, it is easy to establish an optimal solution with a quadratic function since it has only one extreme point (maximum or minimum). Using the objective function $J(u_1, u_2, u_3)$, the aim is to reduce the contaminated maize kernels, livestock and humans alongside the minimization of costs for controls, $u_1(t), u_2(t)$, and $u_3(t)$. We search the optimal control solutions $u_1^*(t), u_2^*(t)$, and $u_3^*(t)$ such that;

$$J(u_1^*, u_2^*, u_3^*) = min\{J(u_1, u_2, u_3) | u_1, u_2, u_3 \in \mathbf{u}\}. \tag{21}$$

where, $\mathbf{u} = \{u_1, u_2, u_3\}$ is an admissible control set so that u_1, u_2, and u_3 are measurable with $0 \leq u_1 \leq 1$, $0 \leq u_2 \leq 1$, and $0 \leq u_3 \leq 1$, for $t \in [0, t_f]$.

4.2. Characterization of the optimal control

We apply Pontryagin's maximum principle [73] which provides the necessary conditions that an optimal control problem must satisfy. The principle converts system (1) and Eq. (20) to a point-wise minimization problem of a Hamiltonian H, with respect to u_1, u_2, and u_3 given by;

$$\begin{aligned} H =& A_1 C_C + A_2 C_L + A_3 A + A_4 C_H + \frac{C_1 u_1^2}{2} + \frac{C_2 u_2^2}{2} + \frac{C_3 u_3^2}{2} \\ &+ \lambda_1(\pi_C - ((1-u_1(t))\beta_1 A + \omega_1 + \mu_C) S_C) \\ &+ \lambda_2((1-u_1(t))\beta_1 A S_C - (\omega_1 + \mu_C) C_C) \\ &+ \lambda_3(\pi_L - ((1-u_3(t))\beta_2 C_C + \mu_L) S_L) \\ &+ \lambda_4((1-u_3(t))\beta_2 C_C S_L - (\mu_L + \phi_L) C_L) \\ &+ \lambda_5(\pi_H - ((1-u_3(t))(\beta_4 C_C + \beta_5 C_L) + \mu_H) S_H) \\ &+ \lambda_6((1-u_3(t))(\beta_4 C_C + \beta_5 C_L) S_H - (\mu_H + \phi_H) C_H) \\ &+ \lambda_7(\rho C_C - (1+u_2)\alpha A) \end{aligned} \tag{22}$$

where λ_1, λ_2, λ_3, λ_4, λ_5, λ_6, and λ_7 are the adjoint or co-state variables. The adjoint equations are obtained by $\frac{d\lambda_i}{dt} = -\frac{\partial H}{\partial V_i}$ with transversality condition $\lambda_i(t_f) = 0$ and V_i represent model variables.

From Eq. (22), we obtain the following adjoint equations;

$$\begin{aligned} \frac{\partial \lambda_1}{\partial t} &= \lambda_1\left((1-u_1)\beta_1 A + \omega_1 + \mu_C\right) - \lambda_2\left((1-u_1)\beta_1 A\right), \\ \frac{\partial \lambda_2}{\partial t} &= -A_1 + \lambda_2(\omega_1 + \mu_C) + \lambda_3((1-u_3)\beta_2 S_L) - \lambda_4((1-u_3)\beta_2 S_L) + \lambda_5((1-u_3)\beta_4 S_H) \\ &\quad - \lambda_6((1-u_3)\beta_4 S_H) - \lambda_7 \rho, \\ \frac{\partial \lambda_3}{\partial t} &= \lambda_3((1-u_3)\beta_2 C_C - \mu_L) - \lambda_4((1-u_3)\beta_2 C_C), \\ \frac{\partial \lambda_4}{\partial t} &= -A_2 + \lambda_4(\mu_L + \phi_L) + \lambda_5((1-u_3)\beta_5 S_H) - \lambda_6((1-u_3)\beta_5 S_H), \end{aligned} \tag{23}$$

$$\frac{\partial \lambda_5}{\partial t} = \lambda_5((1-u_3)(\beta_4 C_C + \beta_5 C_L) - \mu_H) - \lambda_6((1-u_3)(\beta_4 C_C + \beta_5 C_L)),$$
$$\frac{\partial \lambda_6}{\partial t} = -A_4 + \lambda_6(\mu_H + \phi_H),$$
$$\frac{\partial \lambda_7}{\partial t} = -A_3 + \lambda_7((1+u_2)\alpha).$$

The optimality of the control problem is obtained from Eq. (22) as $u_i^* = \frac{\partial H}{\partial u_i} = 0$ where $i = 1, 2, 3$ so that

$$\begin{aligned}
\frac{\partial H}{\partial u_1} &= C_1 u_1 + \lambda_1 \beta_1 A S_C - \lambda_2 \beta_1 A S_C, \\
\frac{\partial H}{\partial u_2} &= C_2 u_2 - \lambda_7 \alpha A, \\
\frac{\partial H}{\partial u_3} &= C_3 u_3 + \lambda_3 \beta_2 C_C S_L - \lambda_4 \beta_2 C_C S_L + \lambda_5(\beta_4 C_C S_H + \beta_5 C_L S_H) - \lambda_6(\beta_4 C_C S_H + \beta_5 C_L S_H).
\end{aligned} \tag{24}$$

The solution of $u_1^*(t)$, $u_2^*(t)$ and $u_3^*(t)$ are presented in compact form as

$$\begin{aligned}
u_1^*(t) &= max\left\{0, min\left\{1, \frac{\lambda_2 \beta_1 A S_C - \lambda_1 \beta_1 A S_C}{C_1}\right\}\right\}, \\
u_2^*(t) &= max\left\{0, min\left\{1, \frac{\lambda_7 \alpha A}{C_2}\right\}\right\}, \\
u_3^*(t) &= max\left\{0, min\left\{1, \frac{\lambda_6[\beta_4 C_C S_H + \beta_5 C_L S_H] + \lambda_4 \beta_2 C_C S_L - \lambda_5 M - \lambda_3 \beta_2 C_C S_L}{C_3}\right\}\right\},
\end{aligned} \tag{25}$$

where $M = \beta_4 C_C S_H + \beta_5 C_L S_H$.

Therefore, the optimal control problem is defined as

$$J(u_1^*, u_2^*, u_3^*) = min\{J(u_1, u_2, u_3) | u_1, u_2, u_3 \in \mathbf{u}\}$$

subject to (1) and (2).

5. Numerical simulation

In this section, the numerical effects of optimal control strategies are analyzed and discussed. The optimal control solution is found through solving the optimality system that comprises of the adjoint system (23) and the state system (1). The Fourth-order Runge–Kutta iterative scheme method was used in solving the state equations with an initial estimate for the controls over the simulated time. The Fourth-order Runge–Kutta method is a fourth-order method with a truncation error of $O(h^5)$, where h is the step size. This means that the error in each step is proportional to h^5, making the method very accurate [74]. In terms of stability, the Fourth-order Runge–Kutta method is designed to be stable for a wide range of problems and is generally considered to be very stable [74]. The rate of convergence for the Fourth-order Runge–Kutta method is $O(h^4)$, which means that the error in the numerical solution decreases rapidly as the step size is decreased [74]. The backward fourth-order Runge–Kutta scheme was used in solving the adjoint equations by utilizing the existing solutions of the state equations due to the transversality conditions (23). Additionally, the convex combination of the prior controls and the value from the characterizations (25) are applied in updating the controls. The procedure is repeated and the iterations are terminated once the values of unknowns at the preceding iterations are so close to the ones at the current iteration [44,75].

Values used for numerical simulation are shown in Table 3. To obtain the assumed values, we have taken data from Dodoma region in Tanzania which is estimated to have $2,500,000$ people and $1,500,000$ cattle [76–78]. The life span of humans in Tanzania is about 66 years [76]. Thus, death rate of humans is estimated to be, $\mu_H = \frac{1}{66} = 0.015$ while the recruitment rate is estimated as, $\pi_H = 2,500,000 \times 0.015 = 37{,}500$. On the other hand, the life span of cattle is estimated to be 6 years [79], therefore we can estimate the death rate of cattle to be $\mu_H = \frac{1}{6} = 0.017$ and the recruitment rate $\pi_H = 1,500,000 \times 0.017 = 255,000$. Furthermore, it is estimated that Dodoma region produces 180,000 tonnes of maize per year [77] while 25% of it is lost during or after harvest [80,81]. Therefore, we estimate the maize recruitment rate, $\pi_C = 180,000$, maize loss rate, $\mu_C = 0.25$ and the maize consumption rate, $\omega_1 = 0.75$ assuming that all maize produced are consumed within a year. The initial values used in this study are $[S_C(0)\ C_C(0)\ S_L(0)\ C_L(0)\ S_H(0)\ C_H(0)\ A(0)] = [180,000\ 0\ 1,5000,000\ 0\ 2,500,000\ 0\ 18000]$. The initial values for susceptible populations are recruitment rates, while for contaminated populations, they are assumed to be zero. Since all contamination starts with fungi, a nominal value of 18,000 aflatoxin fungi was assumed to be the initial value.

Due to inadequate information on estimating the weights, we theoretically choose weights to be $A_3 = 0.8$, $A_1 = 0.7$, $A_2 = 0.6$, $A_4 = 0.5$ and the costs to be $C_2 = 5$, $C_1 = 4$ and $C_3 = 3$ just for illustration purpose in this paper. We assume that more effort should be given to reduce aflatoxin fungi in soil (biological control) followed by reducing crop's contamination rate (good agricultural practices) and lastly livestock and human contamination (public education and awareness) such that $A_3 > A_1 > A_2 > A_4$. The aim is to put more emphasis on the main source of aflatoxin by stopping infection process as suggested by other researchers [34,82]. In the next subsections, we present results of the control strategies simulated over (t_f) ten years. Strategies have been ranked in order of effectiveness in reducing contamination, beginning with the least effective and progressing to the most effective.

Table 3
Description of parameters used in numerical simulations.

Parameter	Value	Source
β_1	0.05	[83]
β_2	0.003	[84]
β_4	0.002	[84]
β_5	0.001	[84]
ρ	0.019	[1]
π_C	180,000	See text
π_L	255,000	See text
ϕ_L	0.2	[85]
ϕ_H	0.1	[12]
ω_1	0.75	[40]
α	0.1	[84]
π_H	37,500	See text
μ_L	0.17	See text
μ_H	0.015	See text
μ_C	0.25	See text

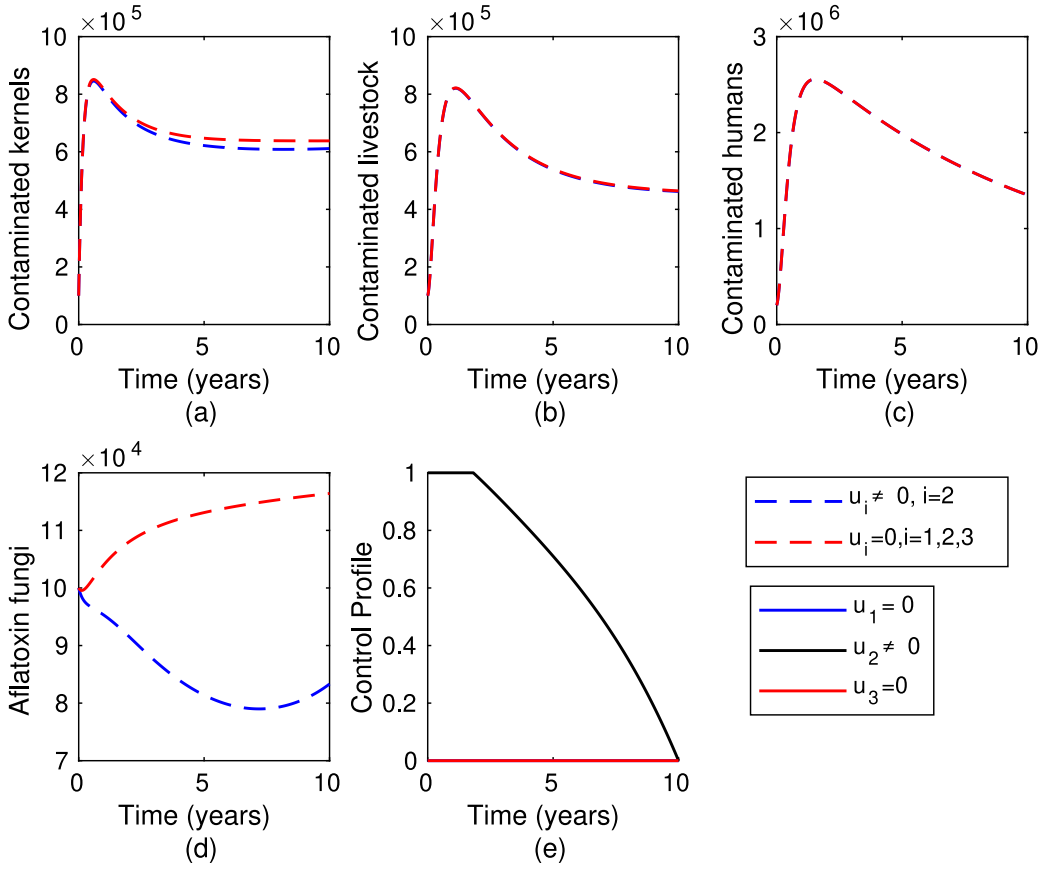

Fig. 2. Impact of Biological control on contaminated maize kernels, livestock, humans and aflatoxin fungi.

5.1. Strategy Q: Biological control

This strategy focuses on eliminating or reducing aflatoxin fungi in soil using biological control $u_2(t)$. Simulation shows that it reduces aflatoxin fungi significantly in seven years but this benefit cannot be sustained until the final time (Fig. 2(d)). It also reduce a very small portion of contaminated maize kernels (Fig. 2(a)). However, it does not reduce contaminated livestock and humans as shown in Fig. 2(b) and Fig. 2(c) respectively. With this strategy biological control $u_2(t)$ is applied at 100% in the first two years and gradually decreasing to zero in the tenth year as shown by control profile in Fig. 2(e).

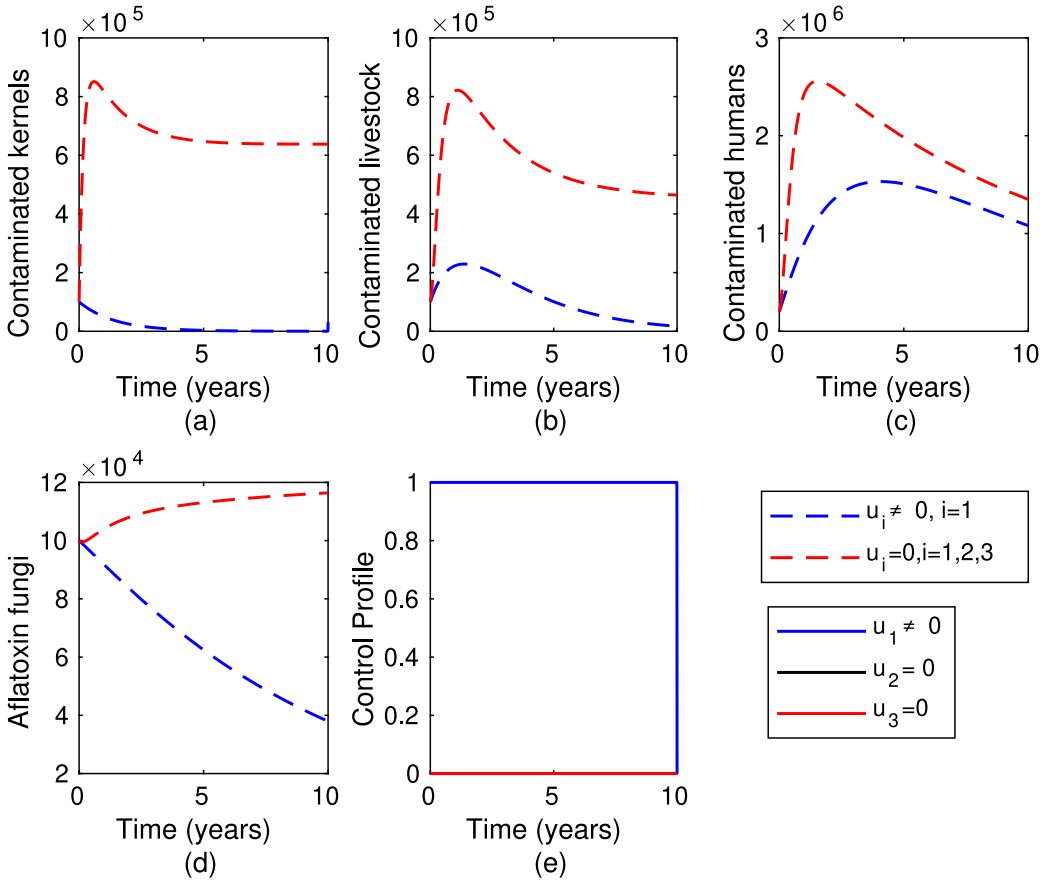

Fig. 3. Impact of Good farming practices on contaminated maize kernels, livestock, humans and aflatoxin fungi.

5.2. Strategy P: Good farming practices

In this strategy we consider good farming practices $u_1(t)$ as the only control to be implemented. Simulations show that contaminated maize kernels decreases to zero in less than five years. However, a larger portion of contaminated livestock, human and aflatoxin fungi remain at the final time as shown in Fig. 3(b), 3(c) and 3(c) indicating that strategy P does not fully eliminate aflatoxin contamination in population. With this strategy good farming practices $u_1(t)$ should be fully implemented throughout the entire period (10 years) as shown by control profile in Fig. 3(e).

5.3. Strategy R: Public education and awareness campaigns

This strategy considers public education and awareness campaigns $u_3(t)$ as the only control to be implemented. Simulations show that it reduces contaminated livestock and humans nearly to zero as shown by Fig. 4(b) and Fig. 4(c) respectively. However, this strategy does not reduce contaminated maize kernels and aflatoxin fungi and they remain the same as shown by Fig. 4(a) and 4(d). With this strategy public education and awareness campaigns $u_3(t)$ should be fully implemented throughout the entire period (10 years) as shown by control profile in Fig. 4(e).

5.4. Strategy S: Good farming practices and biological control

This strategy considers the combination of good farming practices $u_1(t)$ and biological control $u_2(t)$. Fig. 5 shows that contaminated maize kernels and livestock decreases to zero after 5 and 10 years respectively. However, some portion of contaminated human and aflatoxin fungi remain at the final time as shown in Fig. 5(c) indicating that strategy S does not fully eliminate aflatoxin contamination in human population. With this strategy good farming practices $u_1(t)$ should be fully implemented throughout the entire period (10 years) while biological control $u_2(t)$ starts at fully in the first two years and then gradually decreases to zero as shown by control profile in Fig. 5(e).

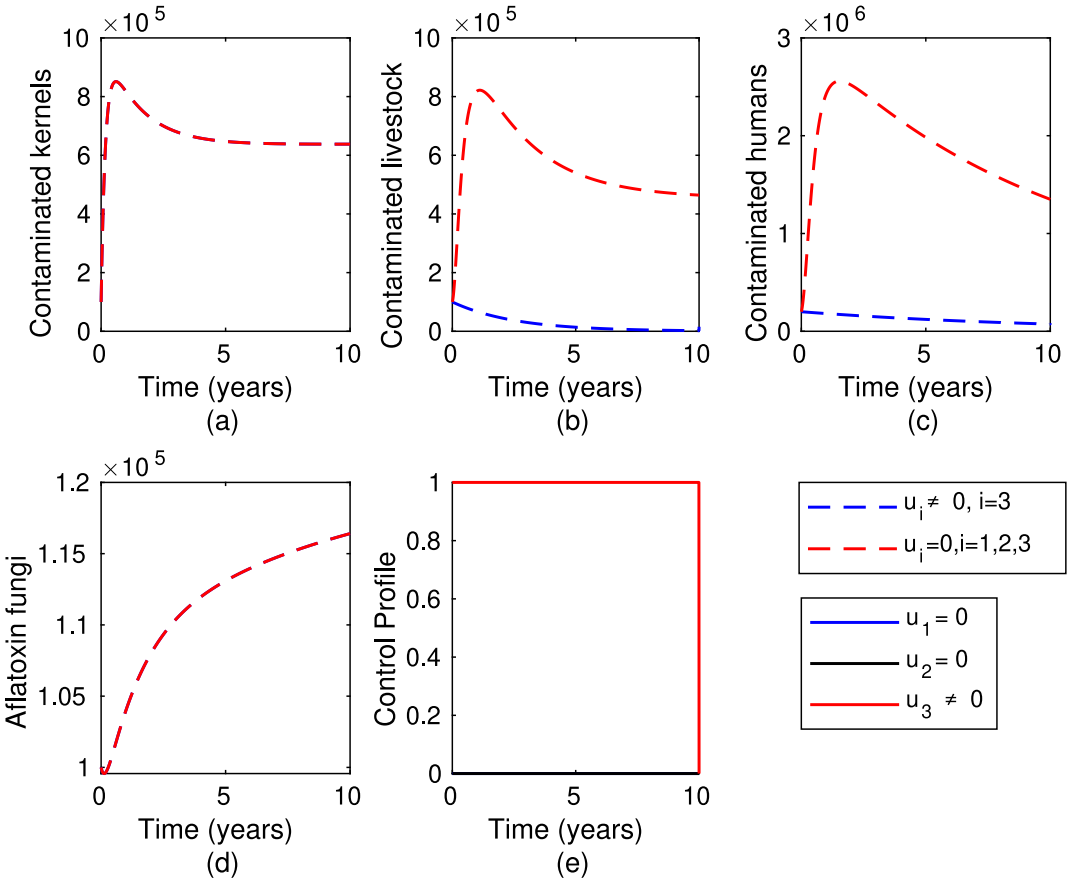

Fig. 4. Impact of public education and awareness campaigns on contaminated maize kernels, livestock, humans and aflatoxin fungi.

5.5. Strategy T: Good farming practices and public education and awareness campaigns

This strategy considers the combination of good farming practices $u_1(t)$ and public education and awareness campaigns $u_3(t)$. Fig. 6 shows that contaminated maize kernels and livestock decreases to zero after 4 and 6 years respectively. Aflatoxin fungi has shown a gentle decrease but does not reach zero in 10 years as shown by Fig. 6(d). Contaminated human decreases and approaches zero at the final time as shown in Fig. 6(c) indicating that strategy T can fully eliminate the aflatoxin contamination. With this strategy good farming practices $u_1(t)$ should be fully implemented throughout the entire period (10 years) while public education and awareness campaigns $u_3(t)$ should be fully implemented for almost 8 years and decreases to zero as shown by control profile in Fig. 6(e).

5.6. Strategy U: Biological control and public education and awareness campaigns

This strategy considers the combination of biological control $u_2(t)$ and public education and awareness campaigns $u_3(t)$. Fig. 7 shows that contaminated livestock and humans decreases to zero after 7 and 9 years respectively. Aflatoxin fungi has shown a gentle decrease in first five years before starting to increase again as shown by Fig. 7(c). However, a large portion of contaminated maize kernels remains at the final time as shown in Fig. 7(a) indicating that strategy U does not fully eliminate aflatoxin contamination in crop population. With this strategy public education and awareness campaigns $u_3(t)$ should be fully implemented throughout the entire period (10 years) while biological control $u_2(t)$ should start at fully in the first two years and gradually decreasing to zero in the tenth year as shown by control profile in Fig. 7(e).

5.7. Strategy V: Good farming practices, biological control and public education and awareness campaigns

This strategy consider the combination of all controls: good farming practices $u_1(t)$, biological control $u_2(t)$ and public education and awareness campaigns $u_3(t)$. Fig. 8 shows that contaminated maize kernels and livestock decreases to zero after 3 and 6 years respectively. Contaminated humans also decreases to nearly zero while aflatoxin fungi showing gradual decrease though it does not

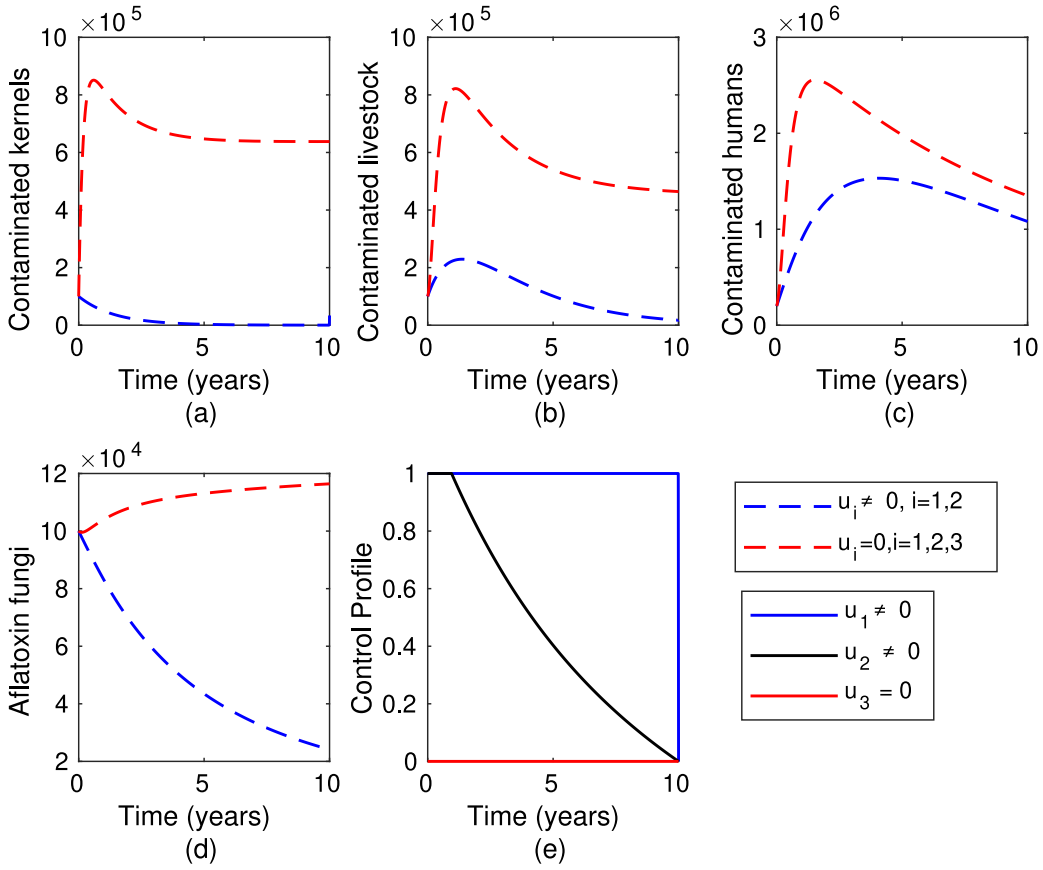

Fig. 5. Impact of Good farming practices and Biological control on contaminated maize kernels, livestock, humans and aflatoxin fungi.

reach zero in 10 years. Although this strategy does not full eliminate aflatoxin fungi in ten years, it has shown good impacts in all populations. With this strategy good farming practices $u_1(t)$ should be full applied throughout the entire period, public education and awareness campaigns $u_3(t)$ full implemented for 8 years while biological control $u_2(t)$ starts at 100% and gradually decreases to zero as shown by control profile in Fig. 8(e).

We also did a sensitivity analysis of the computed controls with respect to parameters and the results are shown in Fig. 9. For sensitivity, we exclude recruitment and mortality rates parameters. We aim to see how controls vary when values of parameters uniformly change from the baseline. Good farming practices (u_1) do not change much with changes in crop contamination rate (β_1). With all values of β_1 (0.05, 0.0375 and 0.025), good farming practices (u_1) should be fully applied until 9 to 10 years as shown in Fig. 9(a). Biological control (u_2) was very sensitive, with 10%, 60% and 70% for 0.075, 0.1 and 0.125 values of reduction rate of aflatoxin fungi in soil (α) respectively as shown in Fig. 9(b). On the other hand, public education and awareness campaign was more sensitive to changes in livestock contamination rate (β_2), followed by human contamination rate from maize kernels (β_4) and was less sensitive to human contamination rate from livestock (β_5) as shown in Fig. 9(c), 9(d) and 9(e) respectively.

6. Cost-effectiveness analysis

The cost effectiveness analysis helps to show the economic benefit for the control strategies. It is used to make comparison between the relative costs and outcomes of different strategies [45]. In this section, we carry out a cost-effectiveness analysis to justify the costs associated with control strategies: P, Q, R, S, T, U and V. The analysis is based on incremental cost-effectiveness ratio (ICER), which is given by;

$$ICER \text{ for } X = \frac{\text{Cost of Strategy } X - \text{Cost of Strategy } Y}{\text{Effect of Strategy } X - \text{Effect of Strategy } Y} \tag{26}$$

whereby X and Y correspond to the strategic interventions being compared in the present case. Using the simulation results, the control strategies are ranked in increasing order of effectiveness based on cases of contamination averted as shown by Table 4. Their corresponding total cost and ICER values for control strategies are also given in Table 4. The ICER values are computed by dividing difference in cost between two strategies by their difference in contamination averted as shown in Eq. (26). Generally, ICER value represent the additional cost per additional health outcome.

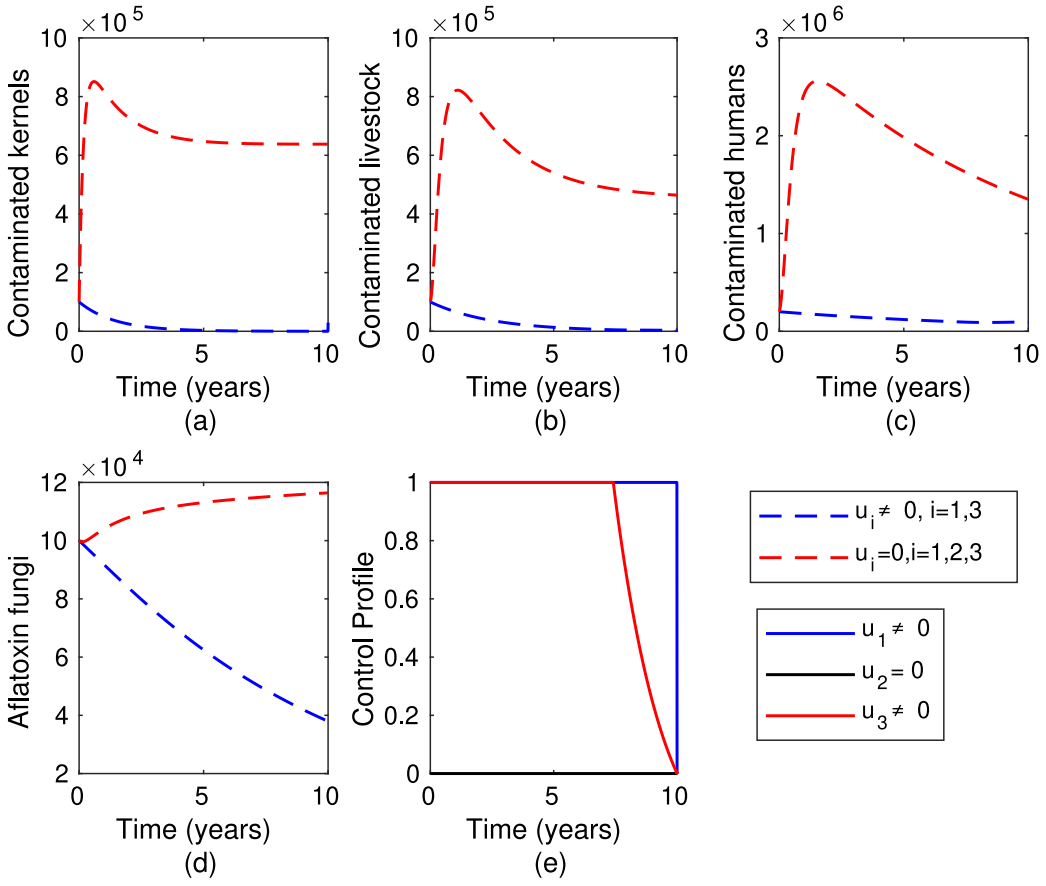

Fig. 6. Impact of Good farming practices and Public education and awareness campaigns on contaminated maize kernels, livestock, humans and aflatoxin fungi.

Table 4
ICER for P, Q, R, S, T, U and V control strategies.

Strategy	Total contamination averted	Total cost ($)	ICER value
Strategy Q	148520	8999300	60.593186
Strategy P	10306000	3420300	−0.549250
Strategy S	10350000	3394200	−0.593182
Strategy R	13363000	3883500	0.162396
Strategy U	13517000	3720700	−1.057143
Strategy T	17559000	700960	−0.747091
Strategy V	17608000	669230	−0.647551

Table 5
ICER for T and V control strategies.

Strategy	Total contamination averted	Total cost ($)	ICER value
Strategy T	17559000	700960	0.039920
Strategy V	17608000	669230	−0.647551

According to results in Table 4, strategy Q has highest ICER values indicating that it is more costly and under-achieving strategy compared to others. As such it is removed from the batch of options to preserve the available limited resources. Same procedures for calculating ICER values are repeated and the final results are presented in Table 5.

Results in Table 5 shows that strategy T has highest ICER values indicating that it is more costly and under-achieving strategy compared to strategy V. We remove strategy T from the batch of options remaining with strategy V. This means that Strategy V is less costly and more effective to implement compared to Strategy T. Thus, these results indicate that strategy V that involves good farming practices, biological control and public education and awareness campaigns saves more money and gives the best

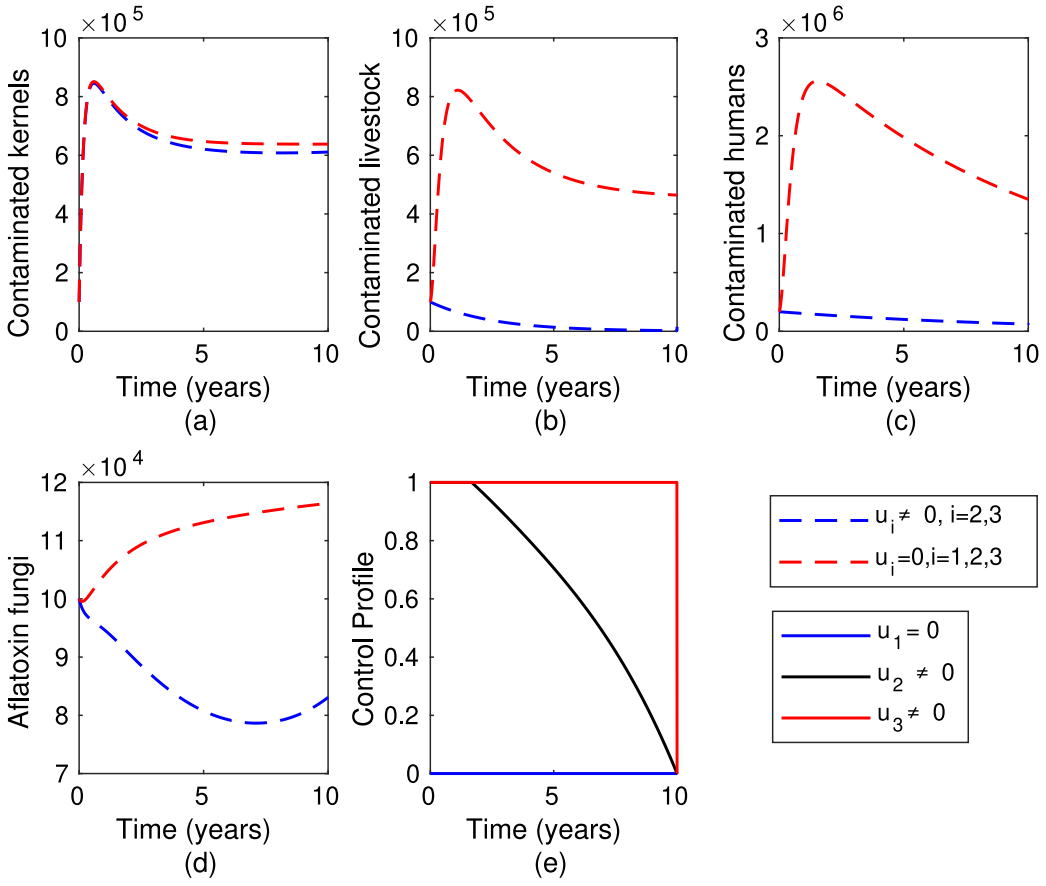

Fig. 7. Impact of Biological control and Public education and awareness campaigns on contaminated maize kernels, livestock, humans and aflatoxin fungi.

outcomes. Therefore, this strategy is the most cost-effective strategy in combating aflatoxin contamination in humans, livestock and maize kernels.

7. Conclusion

In this paper, a deterministic model was developed and analyzed for studying the impact of implementing three time-dependent controls on the dynamics and control of aflatoxin contamination in maize kernels, livestock and humans. The controls that were administered are good farming practices, biological control and public education and awareness campaigns. The optimal control theory was used to find the necessary conditions for the existence of optimal controls and to determine the optimal strategy for controlling the aflatoxin contamination. The cost-effectiveness analysis has also been carried out through the incremental cost effective ratio (ICER) to obtain the most effective strategy. Simulation results for the optimal control problem suggest that a strategy that involves the implementation of all controls is more cost-effective compared to other strategies for controlling aflatoxin contamination in maize kernels, livestock and humans. Therefore, to control aflatoxin contamination, initiatives should focus on good farming practices, biological control and public education and awareness campaigns. These results are similar with other studies in aflatoxin contamination management in terms of recommendations for strategies to be adopted [31,34,82,86] but they suggested quantifying the controls and cost effectiveness analysis. Compared to [40] results, which used only probiotics as a control, our study provides simulations of three controls for preventing aflatoxin contamination. It also provides a cost-effectiveness analysis for the control strategies to help policy-makers in their decision-making. However, in this study, more weight was given to reducing aflatoxin fungi in the environment (biological control), followed by reducing crop's contamination rate (good agricultural practices), and lastly, livestock and human contamination (public education and awareness). This is based on the assumption that controlling aflatoxin contamination from the source (aflatoxin fungi) is more significant [34]. Therefore, results could be different if this assumption is not taken into consideration. Future studies can explicitly look at pre- and post-harvest contamination. They can also extend the model by incorporating the environmental and shading recruitment rates of aflatoxin fungi in soil. Furthermore,

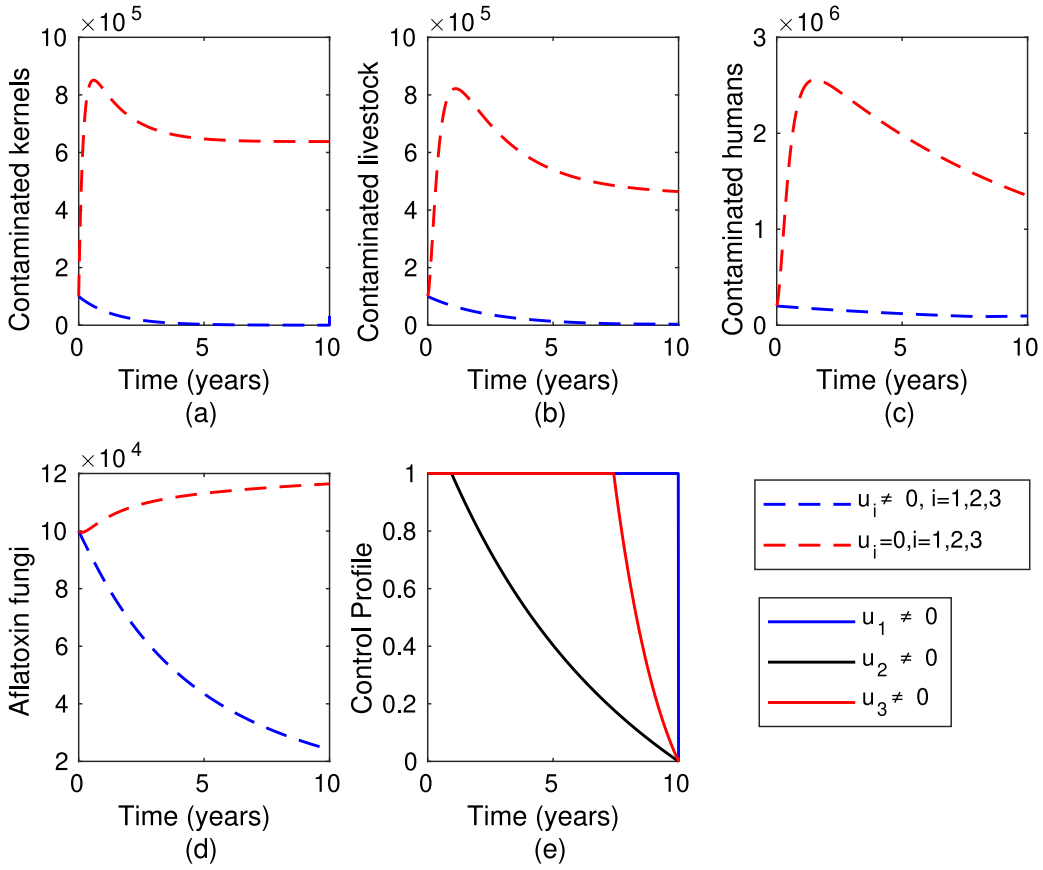

Fig. 8. Impact of Good farming practices, Biological control and Public education and awareness campaigns on contaminated maize kernels, livestock, humans and aflatoxin fungi.

future work can extend the model by incorporating weather fluctuations and climate change, as they are important in aflatoxin fungi's life cycle and aflatoxin formation.

CRediT authorship contribution statement

F.A. Mgandu: Conceptualization, Methodology, Writing – original draft, Writing – review & editing. **S. Mirau:** Conceptualization, Methodology, Writing – review & editing, Supervision. **N. Nyerere:** Conceptualization, Methodology, Writing – review & editing, Supervision. **F. Chirove:** Conceptualization, Methodology, Writing – review & editing, Supervision.

Declaration of competing interest

The authors declare that they have no known competing financial interests or personal relationships that could have appeared to influence the work reported in this paper.

Data availability

All data used in this study are available in the manuscript

Acknowledgments

This work was supported by Tanzania Initiative for Preventing Aflatoxin Contamination (TANIPAC). F. Chirove was supported by the NRF IPRR grant with grant N0: 132253.

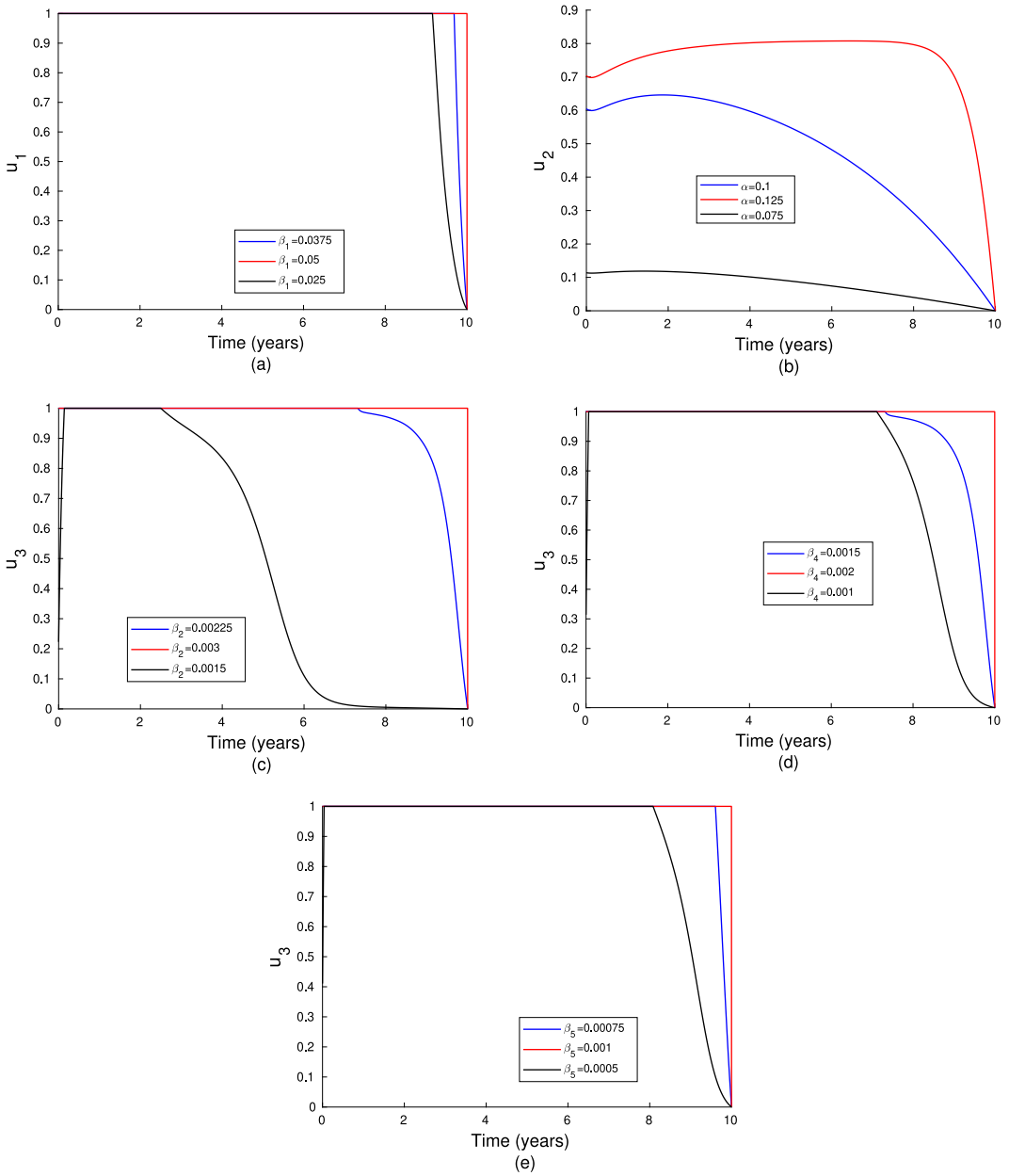

Fig. 9. Sensitivity of computed controls with changes in some parameters.

References

[1] Van der Fels-Klerx HJ, Vermeulen LC, Gavai AK, Liu C. Climate change impacts on aflatoxin B1 in maize and aflatoxin M1 in milk: A case study of maize grown in Eastern Europe and imported to the Netherlands. PLoS One 2019;14(6):1–14.

[2] Oliveira Carlos AF, Corassin Carlos H. Aflatoxins. Future Medicine; 2014.

[3] Dors Giniani Carla, Caldas Sergiane Souza, Feddern Vivian, Bemvenuti Renata Heidtmann, Hackbart HCS, Souza MM, et al. Aflatoxins: contamination, analysis and control. In: Guevara-uolzález RG, editor. Embrapa Suínos e Aves-Capítulo em livro científico. Aflatoxins: biochemistry and molecular …; 2011.

[4] Lahouar Amani, Marin Sonia, Crespo-Sempere Ana, Saïd Salem, Sanchis Vicente. Effects of temperature, water activity and incubation time on fungal growth and aflatoxin B1 production by toxinogenic Aspergillus flavus isolates on sorghum seeds. Rev Argent Microbiol 2016;48(1):78–85.

[5] Astoreca Andrea, Magnoli Carina, Ramirez María L, Combina Mariana, Dalcero Ana. Water activity and temperature effects on growth of Aspergillus niger, A. awamori and A. carbonarius isolated from different substrates in Argentina. Int J Food Microbiol 2007;119(3):314–8.

[6] Kumar Abhishek, Pathak Hardik, Bhadauria Seema, Sudan Jebi. Aflatoxin contamination in food crops: causes, detection, and management: a review. Food Prod Process Nutr 2021;3(1):1–9.

[7] Eshelli Manal, Harvey Linda, Edrada-Ebel RuAngelie, McNeil Brian. Metabolomics of the bio-degradation process of aflatoxin B1 by actinomycetes at an initial pH of 6.0. Toxins 2015;7(2):439–56.
[8] Mushtaq Muhammad, Sultana Bushra, Anwar Farooq, Khan Muhammad Zargham, Ashrafuzzaman Muhammad. Occurrence of aflatoxins in selected processed foods from Pakistan. Int J Mol Sci 2012;13(7):8324–37.
[9] Kamala A, Shirima C, Jani B, Bakari M, Sillo H, Rusibamayila N, et al. Outbreak of an acute aflatoxicosis in Tanzania during 2016. World Mycotoxin J 2018;11(3):311–20.
[10] Iqbal Shahzad Zafar, Nisar Sonia, Asi Muhammad Rafique, Jinap S. Natural incidence of aflatoxins, ochratoxin A and zearalenone in chicken meat and eggs. Food Control 2014;43:98–103.
[11] Su Qun-Ying. The toxification and detoxification mechanisms of aflatoxin B1 in human: An update. In: Aflatoxin B1 occurrence, detection and toxicological effects. IntechOpen; 2019.
[12] Kimanya Martin E, Routledge Michael N, Mpolya Emmanuel, Ezekiel Chibundu N, Shirima Candida P, Gong Yun Yun. Estimating the risk of aflatoxin-induced liver cancer in tanzania based on biomarker data. PLoS One 2021;16(3):e0247281.
[13] Wu Felicia, Groopman John D, Pestka James J. Public health impacts of foodborne mycotoxins. Annu Rev Food Sci Technol 2014;5(1):351–72.
[14] Warnatzsch Erika A, Reay David S, Leggieri Marco Camardo, Battilani Paola. Climate change impact on aflatoxin contamination risk in malawi's maize crops. Front Sustain Food Syst 2020;4:1–13.
[15] Ferlay Jacques, Soerjomataram Isabelle, Dikshit Rajesh, Eser Sultan, Mathers Colin, Rebelo Marise, et al. Cancer incidence and mortality worldwide: sources, methods and major patterns in GLOBOCAN 2012. Int J Cancer 2015;136(5):E359–86.
[16] Liu Yan, Wu Felicia. Global burden of aflatoxin-induced hepatocellular carcinoma: a risk assessment. Environ Health Perspect 2010;118(6):818–24.
[17] European Commissiion. Commission Regulation (EC) No 165/2010 of 26 February 2010, amending Regulation (EC) No 1881/2006setting maximum levels for certain contaminants in foodstuffs as regards aflatoxins. Off J Eur Union 2010;50(2009):8–12.
[18] Gong YY, Routledge M, Kimanya ME, Musoke G, Nelson F, Sonoiya S, et al. Aflatoxin standards for food: Knowledge platform 2015 situational analysis East Africa Region. Build Aflatoxin Safe East Afr Community 2015;1(July):1944–66.
[19] Winter Gal, Pereg Lily. A review on the relation between soil and mycotoxins: Effect of aflatoxin on field, food and finance. Eur J Soil Sci 2019;70(4):882–97.
[20] Xu F, Baker RC, Whitaker TB, Luo H, Zhao Y, Stevenson A, et al. Review of good agricultural practices for smallholder maize farmers to minimise aflatoxin contamination. World Mycotoxin J 2022;15(2):171–86.
[21] Gómez-Salazar Julián Andrés, Ruiz-Hernández Karla, Martínez-Miranda María Marcela, Castro-Ríos Katherin. Postharvest strategies for decontamination of aflatoxins in cereals. Food Rev Int 2021;1–28.
[22] Nji Queenta Ngum, Babalola Olubukola Oluranti, Ekwomadu Theodora Ijeoma, Nleya Nancy, Mwanza Mulunda. Six main contributing factors to high levels of mycotoxin contamination in African foods. Toxins 2022;14(5):318.
[23] Adeyeye SAO, Ashaolu TJ, Idowu-Adebayo F. Mycotoxins: Food safety, consumer health and Africa's food security. Polycycl Aromat Compd 2022;42(8):5779–95.
[24] Chilaka Cynthia Adaku, Obidiegwu Jude Ejikeme, Chilaka Augusta Chinenye, Atanda Olusegun Oladimeji, Mally Angela. Mycotoxin regulatory status in Africa: a decade of weak institutional efforts. Toxins 2022;14(7):442.
[25] Leggieri M Camardo, Lanubile Alessandra, Dall'Asta C, Pietri Amedeo, Battilani Paola. The impact of seasonal weather variation on mycotoxins: Maize crop in 2014 in northern Italy as a case study. World Mycotoxin J 2020;13(1):25–36.
[26] Aristil Junior, Venturini Giovanni, Maddalena Giuliana, Toffolatti Silvia Laura, Spada Alberto. Fungal contamination and aflatoxin content of maize, moringa and peanut foods from rural subsistence farms in South Haiti. J Stored Prod Res 2020;85:101550.
[27] Yao Haibo, Hruska Zuzana, Kincaid Russell, Tao Feifei, Rajasekaran Kanniah. Effect of aspergillus flavus fungi infection and aflatoxin contamination on single corn kernel mechanical strength. Appl Eng Agric 2023;39(2):197–205.
[28] Tao Feifei, Yao Haibo, Zhu Fengle, Hruska Zuzana, Liu Yongliang, Rajasekaran Kanniah, et al. A rapid and nondestructive method for simultaneous determination of aflatoxigenic fungus and aflatoxin contamination on corn kernels. J Agricult Food Chem 2019;67(18):5230–9.
[29] Tembo Elliot. Mycotoxigenic fungi associated with ear-rots in Zimbabwe: Identification and inheritance of resistance in southern and West African maize inbred lines [Ph.D. thesis], University of the Free State; 2015.
[30] Massomo Said MS. Aspergillus flavus and aflatoxin contamination in the maize value chain and what needs to be done in Tanzania. Sci Afr 2020;10:e00606.
[31] Shabeer Saba, Asad Shahzad, Jamal Atif, Ali Akhtar. Aflatoxin contamination, its impact and management strategies: An updated review. Toxins 2022;14(5):307.
[32] Senghor LA, Ortega-Beltran A, Atehnkeng J, Callicott KA, Cotty PJ, Bandyopadhyay Ranajit. The atoxigenic biocontrol product Aflasafe SN01 is a valuable tool to mitigate aflatoxin contamination of both maize and groundnut cultivated in Senegal. Plant Dis 2020;104(2):510–20.
[33] Jallow Abdoulie, Xie Huali, Tang Xiaoqian, Qi Zhang, Li Peiwu. Worldwide aflatoxin contamination of agricultural products and foods: From occurrence to control. Compr Rev Food Sci Food Saf 2021;20(3):2332–81.
[34] Kerstin Hell, Charity Mutegi. Aflatoxin control and prevention strategies in key crops of Sub-Saharan Africa. Afr J Microbiol Res 2011;5(5):459–66.
[35] Pandey Pramila, Pandey Narendra Shankar, Chaturvedi Rachna. Prevention and control strategies of aflatoxin contamination. In: Bio-management of postharvest diseases and mycotoxigenic fungi. CRC Press; 2020, p. 223–34.
[36] Kaale LD, Kimanya ME, Macha IJ, Mlalila N. Aflatoxin contamination and recommendations to improve its control: a review. World Mycotoxin J 2021;14(1):27–40.
[37] Gibellato SL, Dalsóquio LF, do Nascimento ICA, Alvarez TM. Current and promising strategies to prevent and reduce aflatoxin contamination in grains and food matrices. World Mycotoxin J 2021;14(3):293–304.
[38] Battilani P, Camardo Leggieri M, Rossi V, Giorni P. AFLA-maize, a mechanistic model for Aspergillus flavus infection and aflatoxin B1 contamination in maize. Comput Electron Agric 2013;94:38–46.
[39] Dövényi-Nagy Tamás, Rácz Csaba, Molnár Krisztina, Bakó Károly, Szláma Zsombor, Jóźwiak Ákos, et al. Pre-harvest modelling and mitigation of aflatoxins in maize in a changing climatic environment-A review. Toxins 2020;12(12):768.
[40] Kademi Hafizu Ibrahim, Saad Farouk Tijjani, Ulusoy Beyza H, Baba Isa Abdullahi, Hecer Canan. Mathematical model for aflatoxins risk mitigation in food. J Food Eng 2019;263:25–9.
[41] Omame Andrew, Okuonghae Daniel. A co-infection model for oncogenic Human papillomavirus and tuberculosis with optimal control and cost-effectiveness analysis. Optim Control Appl Methods 2021;42(4):1081–101.
[42] Omame Andrew, Abbas Mujahid, Onyenegecha Chibueze P. Backward bifurcation and optimal control in a co-infection model for SARS-CoV-2 and ZIKV. Results Phys 2022;37:105481.
[43] Omame Andrew, Isah Mary Ele, Abbas Mujahid. An optimal control model for COVID-19, zika, dengue, and chikungunya co-dynamics with reinfection. Optim Control Appl Methods 2023;44(1):170–204.
[44] Nyerere Nkuba, Luboobi Livingstone S, Mpeshe Saul C, Shirima Gabriel M. Optimal control strategies for the infectiology of brucellosis. Int J Math Math Sci 2020;2020:1–17.
[45] Mayengo Maranya M. Optimal control model for alcohol–related risk behaviors and beliefs in tanzania. J Appl Math 2022;2022.
[46] Gatyeni SP, Chukwu CW, Chirove Faraimunashe, Nyabadza F, et al. Application of optimal control to the dynamics of COVID-19 disease in South Africa. Sci Afr 2022;16:e01268.

[47] Liu Chongyang, Gong Zhaohua, Yu Changjun, Wang Song, Teo Kok Lay. Optimal control computation for nonlinear fractional time-delay systems with state inequality constraints. J Optim Theory Appl 2021;191(1):83–117.
[48] Liu Chongyang, Loxton Ryan, Teo Kok Lay, Wang Song. Optimal state-delay control in nonlinear dynamic systems. Automatica 2022;135:109981.
[49] Liu Chongyang, Shi Guoqing, Liu Gang, Hu Dianzhong. Optimal control of a nonlinear state-dependent impulsive system in fed-batch process. Int J Biomath 2023;2350001.
[50] Milićević Dragan R, Škrinjar Marija, Baltić Tatjana. Real and perceived risks for mycotoxin contamination in foods and feeds: challenges for food safety control. Toxins 2010;2(4):572–92.
[51] Viegas Susana, Veiga Luisa, Malta-Vacas Joana, Sabino Raquel, Figueredo Paula, Almeida Ana, et al. Occupational exposure to aflatoxin (AFB1) in poultry production. J Toxicol Environ Health A 2012;75(22–23):1330–40.
[52] Yu Jiujiang. Current understanding on aflatoxin biosynthesis and future perspective in reducing aflatoxin contamination. Toxins 2012;4(11):1024–57.
[53] Ramadan Nadeem A, Al-Ameri Hadeel A. Aflatoxins. In: Aflatoxins-occurrence, detoxification, determination and health risks. IntechOpen; 2022.
[54] Norlia Mahror, Jinap Selamat, Nor-Khaizura Mahmud Ab Rashid, Radu Son, Samsudin Nik Iskandar Putra, Azri Farah Asilah. Aspergillus section flavi and aflatoxins: Occurrence, detection, and identification in raw peanuts and peanut-based products along the supply chain. Front Microbiol 2019;10:2602.
[55] Daou Rouaa, Joubrane Karine, Maroun Richard G, Khabbaz Lydia Rabbaa, Ismail Ali, El Khoury André. Mycotoxins: Factors influencing production and control strategies. AIMS Agric Food 2021;6(1):416–47.
[56] Marcianò D, Mizzotti C, Maddalena G, Toffolatti SL, et al. The dark side of fungi: How they cause diseases in plants. Front Young Minds 2021.
[57] Lungu E, Massaro Tyler J, Ndelwa Emmaline, Ainea Neterindwa, Chibaya Symon, Malunguza Noble J. Mathematical modeling of the HIV/Kaposi's sarcoma coinfection dynamics in areas of high HIV prevalence. Comput Math Methods Med 2013;2013.
[58] Huo Hai-Feng, Feng Li-Xiang. Global stability for an HIV/AIDS epidemic model with different latent stages and treatment. Appl Math Model 2013;37(3):1480–9.
[59] Juga M, Nyabadza F, Chirove F. Modelling the impact of stigmatisation of Ebola survivors on the disease transmission dynamics. Sci Rep 2023;13(1):4859.
[60] Diekmann Odo, Heesterbeek Johan Andre Peter, Metz Johan AJ. On the definition and the computation of the basic reproduction ratio R 0 in models for infectious diseases in heterogeneous populations. J Math Biol 1990;28:365–82.
[61] Van den Driessche Pauline, Watmough James. Reproduction numbers and sub-threshold endemic equilibria for compartmental models of disease transmission. Math Biosci 2002;180(1–2):29–48.
[62] Castillo-Chavez Carlos, Blower Sally, Van den Driessche Pauline, Kirschner Denise, Yakubu Abdul-Aziz. Mathematical approaches for emerging and reemerging infectious diseases: models, methods, and theory, vol. 126. Springer Science & Business Media; 2002.
[63] Kamgang Jean Claude, Sallet Gauthier. Global asymptotic stability for the disease free equilibrium for epidemiological models. C R Math 2005;341(7):433–8.
[64] Dumont Yves, Chiroleu Frédéric, Domerg Caroline. On a temporal model for the chikungunya disease: modeling, theory and numerics. Math Biosci 2008;213(1):80–91.
[65] Mwasunda Joshua A, Irunde Jacob I, Kajunguri Damian, Kuznetsov Dmitry. Modeling and analysis of taeniasis and cysticercosis transmission dynamics in humans, pigs and cattle. Adv Difference Equ 2021;2021(1):1–23.
[66] Korobeinikov Andrei, Wake Graeme C. Lyapunov functions and global stability for SIR, SIRS, and SIS epidemiological models. Appl Math Lett 2002;15(8):955–60.
[67] Korobeinikov Andrei. Lyapunov functions and global properties for SEIR and SEIS epidemic models. Math Med Biol 2004;21(2):75–83.
[68] Nyerere Nkuba, Luboobi Livingstone S, Mpeshe Saul C, Shirima Gabriel M. Mathematical model for brucellosis transmission dynamics in livestock and human populations. Communications in Mathematical Biology and Neuroscience; 2020.
[69] Mpeshe Saul C, Haario Heikki, Tchuenche Jean M. A mathematical model of Rift Valley fever with human host. Acta Biotheor 2011;59(3):231–50.
[70] La Salle Joseph P. The stability of dynamical systems. SIAM; 1976.
[71] Li Jianquan, Yang Yali, Zhou Yicang. Global stability of an epidemic model with latent stage and vaccination. Nonlinear Anal RWA 2011;12(4):2163–73.
[72] Nyabadza F, Mukandavire Z, Hove-Musekwa SD. Modelling the HIV/AIDS epidemic trends in South Africa: Insights from a simple mathematical model. Nonlinear Anal RWA 2011;12(4):2091–104.
[73] Pontryagin LS, Boltyanskii VG, Gamkrelidze RV, Mishchenko EF. The maximum principle. In: The mathematical theory of optimal processes. New York: John Wiley and Sons; 1962.
[74] Sauer T. Numerical analysis. 2nd ed. Upper Saddle River: George Mason University, Pearson Education Inc; 2012.
[75] Lenhart Suzanne, Workman John T. Optimal control applied to biological models. CRC Press; 2007.
[76] United Republic of Tanzania. 2012 Population and housing census. Popul Distrib Adm Areas 2013.
[77] Ministry of Agriculture. National sample census of agriculture volume va: Regional report: 2007/2008 dodoma region ministry of agriculture. 2018.
[78] Dietz AJ, Ehrhardt DWL. Tanzania at 60. In: ASCL infosheet. African Studies Centre Leiden (ASCL); 2021.
[79] Michael S, Mbwambo N, Mruttu H, Dotto M, Ndomba C, Silva M da, et al. Tanzania livestock master plan. International Livestock Research Institute; 2018.
[80] Kumar Deepak, Kalita Prasanta. Reducing postharvest losses during storage of grain crops to strengthen food security in developing countries. Foods 2017;6(1):8.
[81] Stathers Tanya, Holcroft Deirdre, Kitinoja Lisa, Mvumi Brighton M, English Alicia, Omotilewa Oluwatoba, et al. A scoping review of interventions for crop postharvest loss reduction in sub-Saharan Africa and South Asia. Nat Sustain 2020;3(10):821–35.
[82] Alshannaq Ahmad F, Gibbons John G, Lee Mi-Kyung, Han Kap-Hoon, Hong Seung-Beom, Yu Jae-Hyuk. Controlling aflatoxin contamination and propagation of Aspergillus flavus by a soy-fermenting Aspergillus oryzae strain. Sci Rep 2018;8(1):1–14.
[83] Chauhan Yashvir, Tatnell Jeff, Krosch Stephen, Karanja James, Gnonlonfin Benoit, Wanjuki Immaculate, et al. An improved simulation model to predict pre-harvest aflatoxin risk in maize. Field Crops Res 2015;178:91–9.
[84] Kademi Hafizu Ibrahim, Baba Isa Abdullahi, Saad Farouk Tijjani. Modelling the dynamics of toxicity associated with aflatoxins in foods and feeds. Toxicol Rep 2017;4:358–63.
[85] Zain Mohamed E. Impact of mycotoxins on humans and animals. J Saudi Chem Soc 2011;15(2):129–44.
[86] Falade Titilayo. Aflatoxin management strategies in sub-Saharan Africa. In: Mycotoxins-impact and management strategies. IntechOpen; 2018.